Efetov Lab
Chair of Quantum Materials

European Research Council erc · European Innovation Council · DFG
Gottfried Wilhelm Leibniz Preis · Munich Quantum Valley · MCQST
THE KAVLI FOUNDATION · Klaus Tschira Stiftung · KEELE FOUNDATION

College de France 13.05.2026

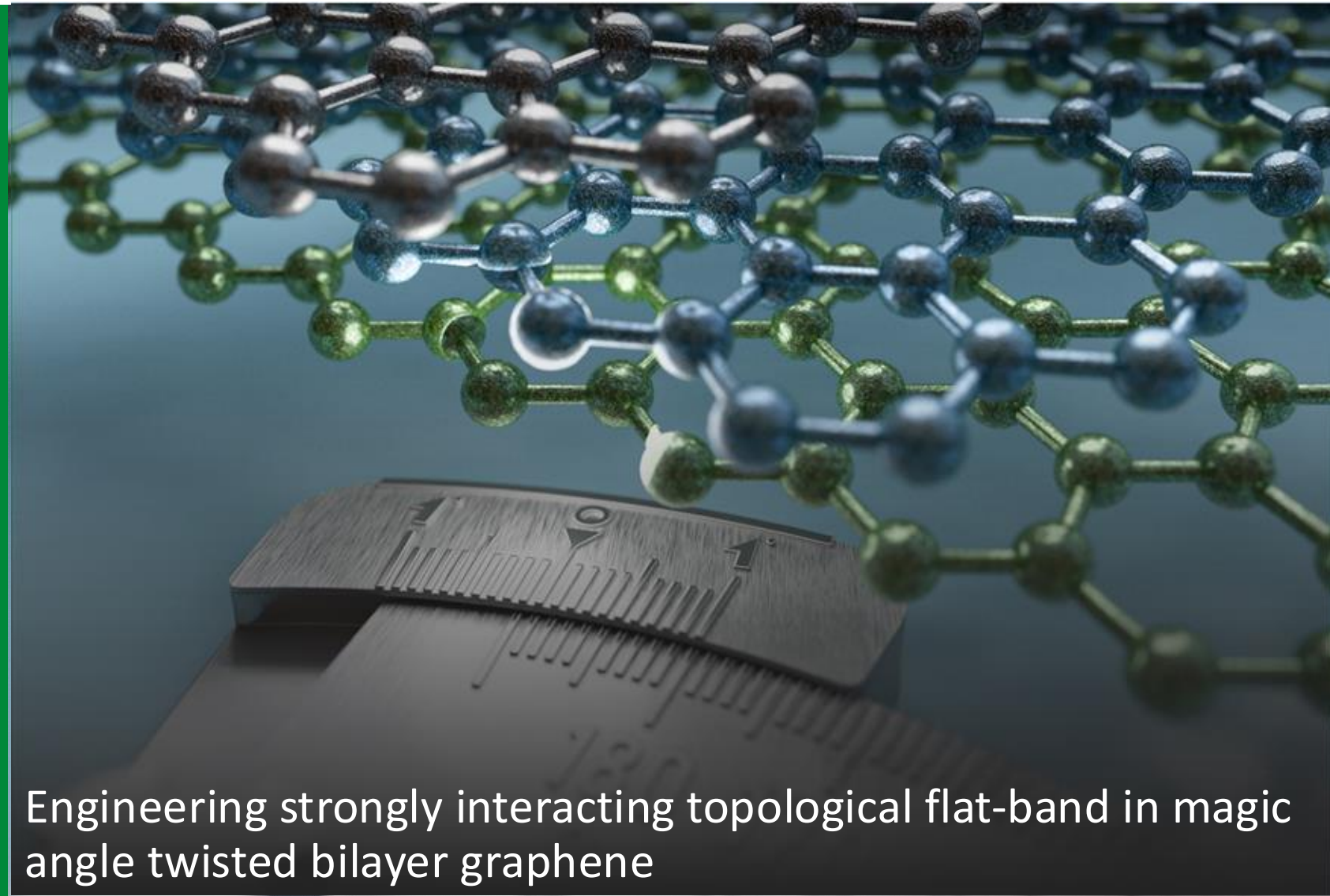

Engineering strongly interacting topological flat-band in magic angle twisted bilayer graphene

Twisting 2D materials - Moiré interference pattern

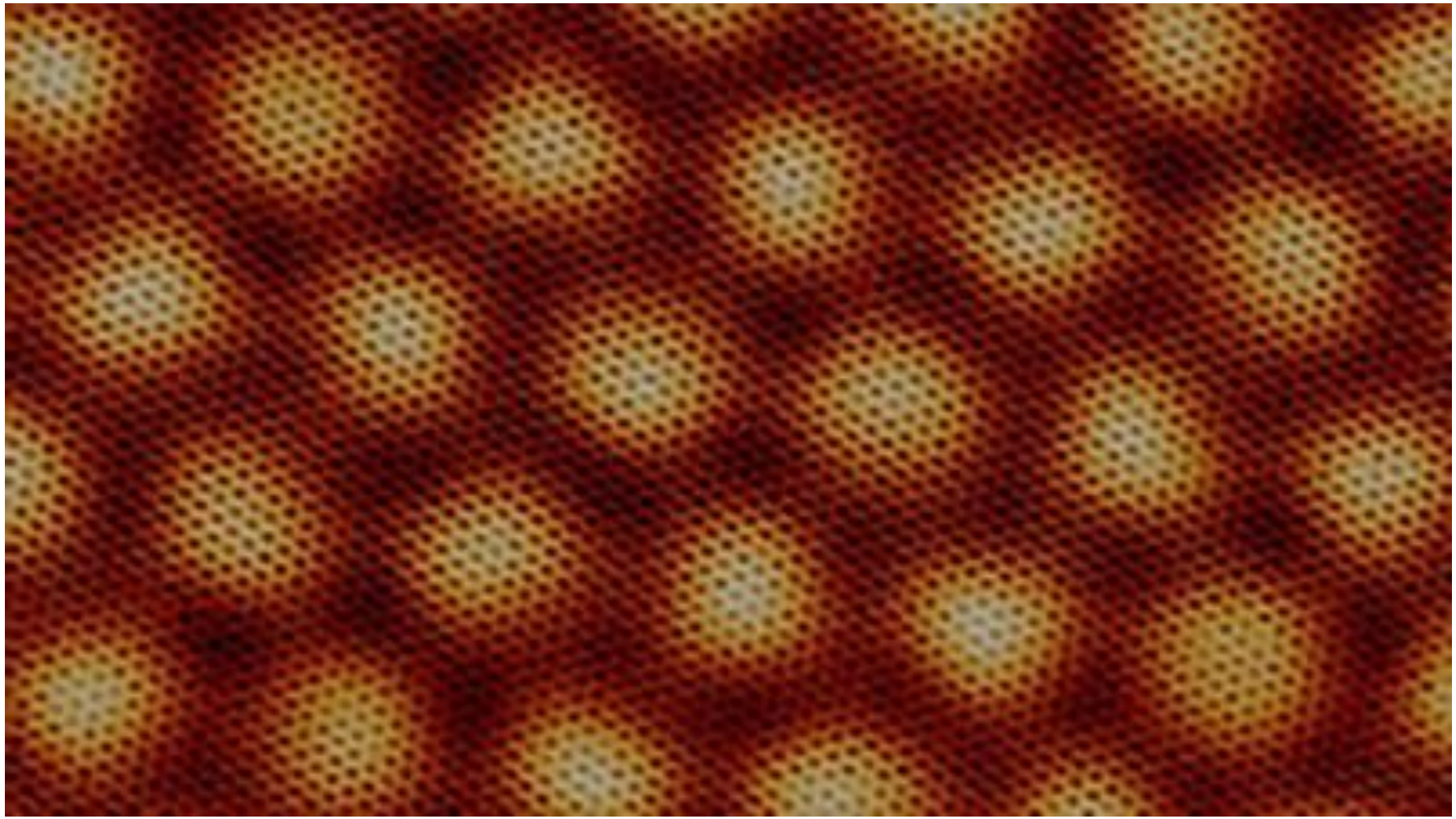

Yazdani group (2023).

Strongly correlated quantum materials

Efetov Lab

Phase diagram of heavy fermion compound:

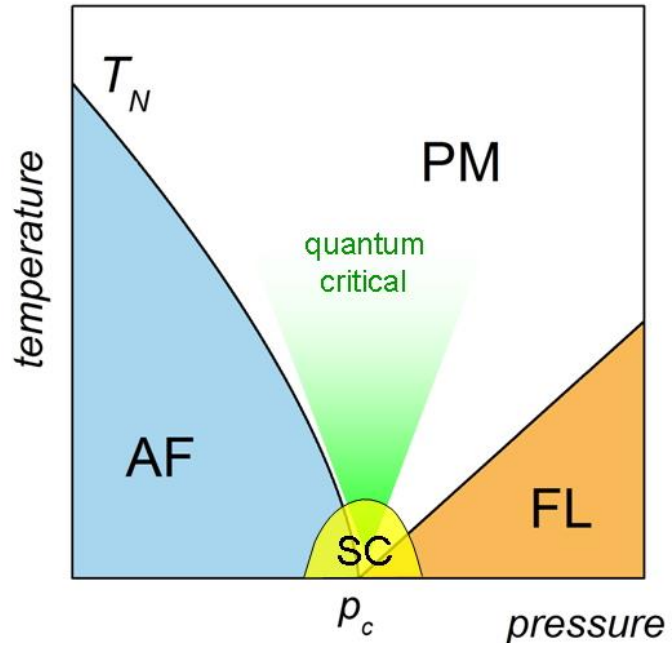

Phase diagrams of fractional quantum Hall:

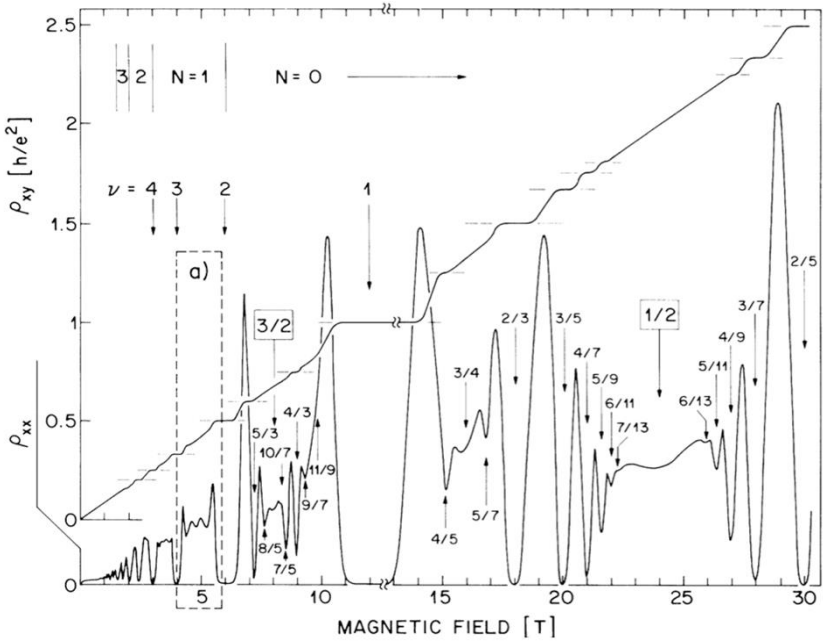

Main principles:

- Interactions between particles dominate.
- Emergence of novel phases (superconductivity, quantum spin liquids, topological states).
- Rich collective behavior and new quasiparticles.

Big open questions:

- What drives high-temperature superconductivity?
- What is the nature of non-Fermi liquid behavior?
- How do entanglement and topology shape quantum matter?

Novel experimental possibilities and control knobs

Efetov Lab

Novel control knobs:

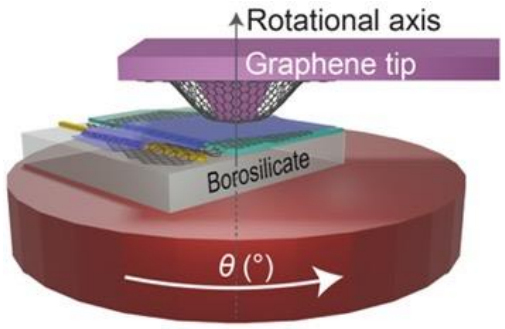

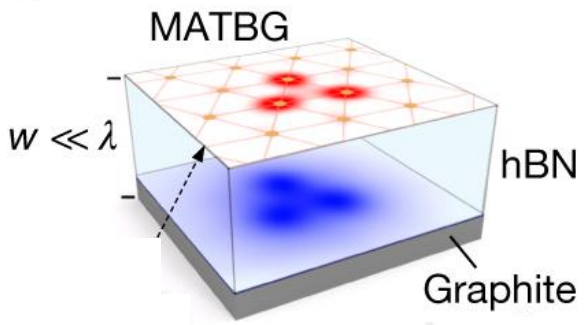

- Twist angle → tunes bandwidth and topology of bands.
- Carrier density (gating/doping) → controls filling and phase transitions.
- Displacement field (dual gates) → modifies symmetry.
- Layer stacking / alignment → changes symmetry, topology, and interactions.
- Dielectric environment → screens interactions and modifies correlation strength.

Novel experimental possibilities::

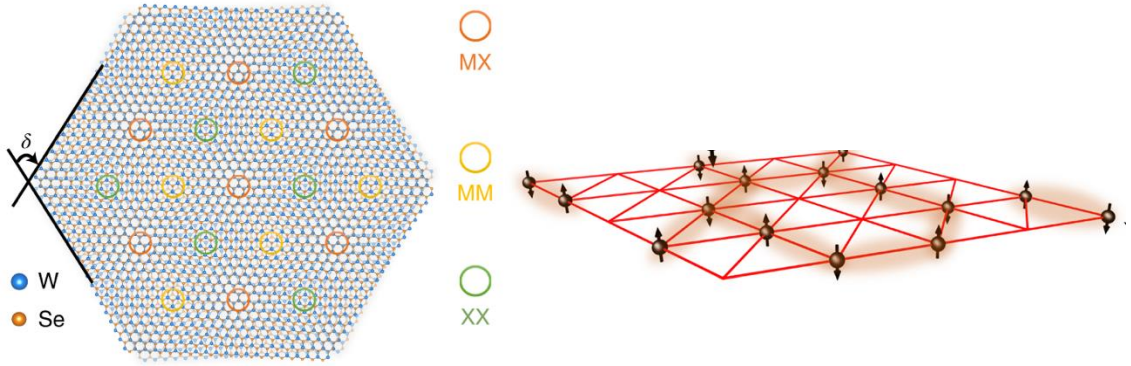

- Realization of tunable Hubbard models in solid-state platforms.
- Access to flat bands → enhanced correlations and emergent phases (SC, Mott, Chern insulators).
- Exploration of topological bands with strong interactions.
- Direct comparison between theory and experiment in a highly controllable setting.

Moiré materials

New platform for strongly correlated electrons

Efetov Lab

Crystals:

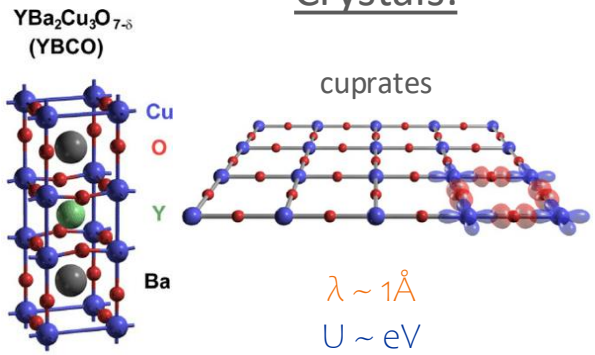

cuprates

λ ~ 1Å

U ~ eV

Magic-angle tBLG:

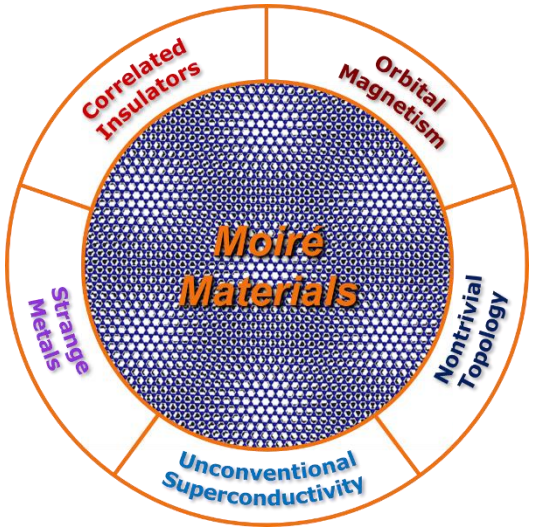

λ ~ 10nm

U ~ meV

Lattice constant

Interaction strength

Optical lattices:

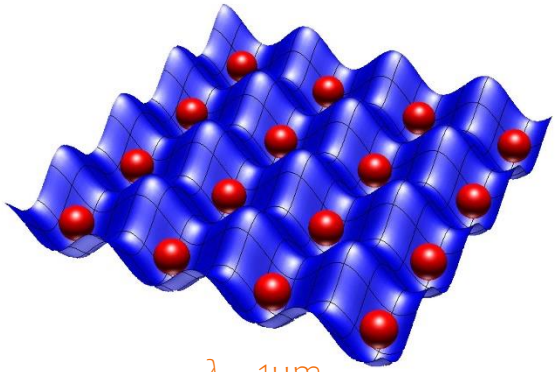

λ ~ 1μm

U ~ peV

LMU LUDWIG-MAXIMILIANS-UNIVERSITÄT MÜNCHEN

Graphene ’04

Efetov Lab

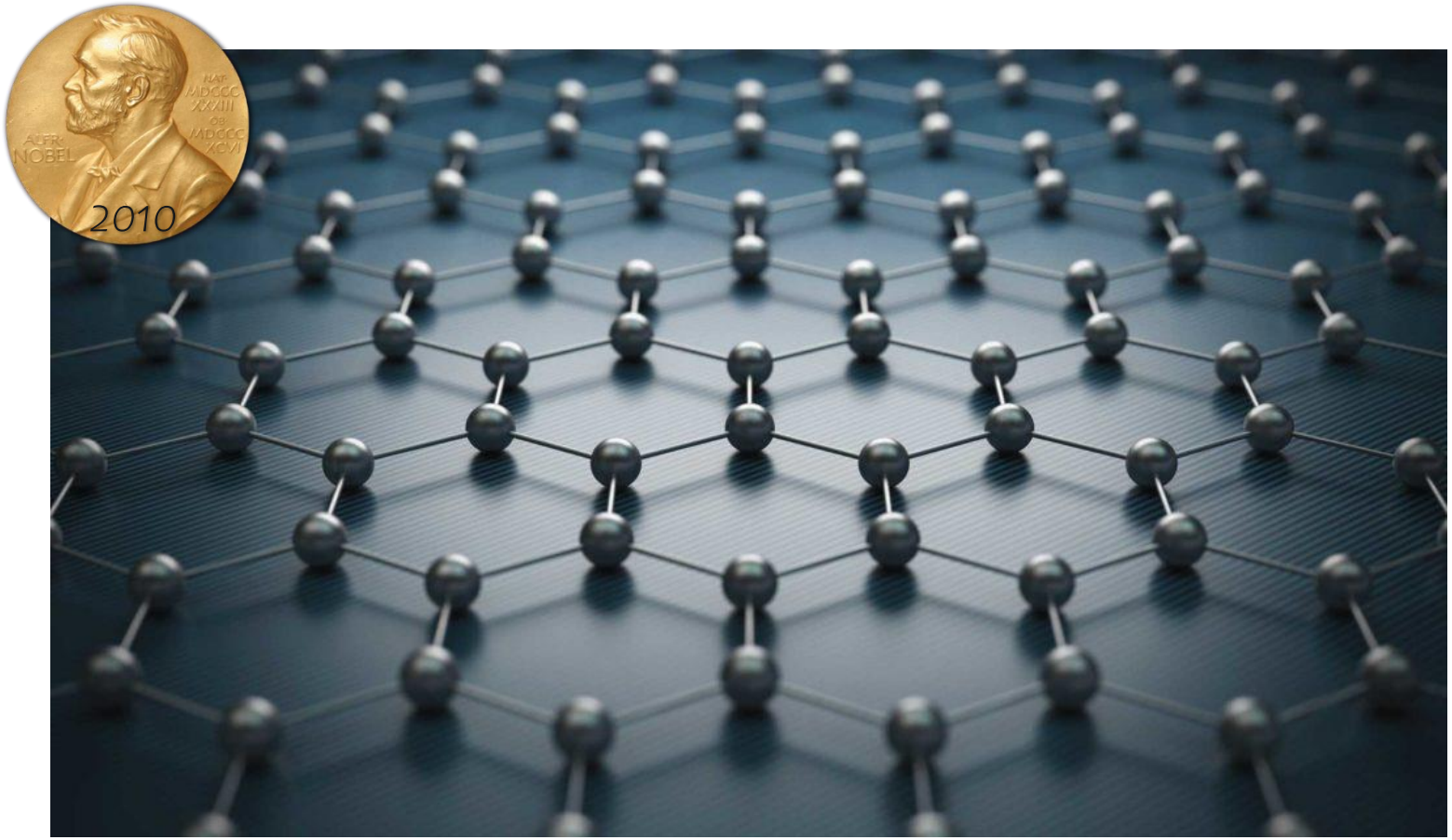

→ One atomic layer of carbon atoms

→ True 2D material

→ Scotch tape

Advent of Graphene and 2D van der Waals materials

Efetov Lab

Graphene 2D lattice:

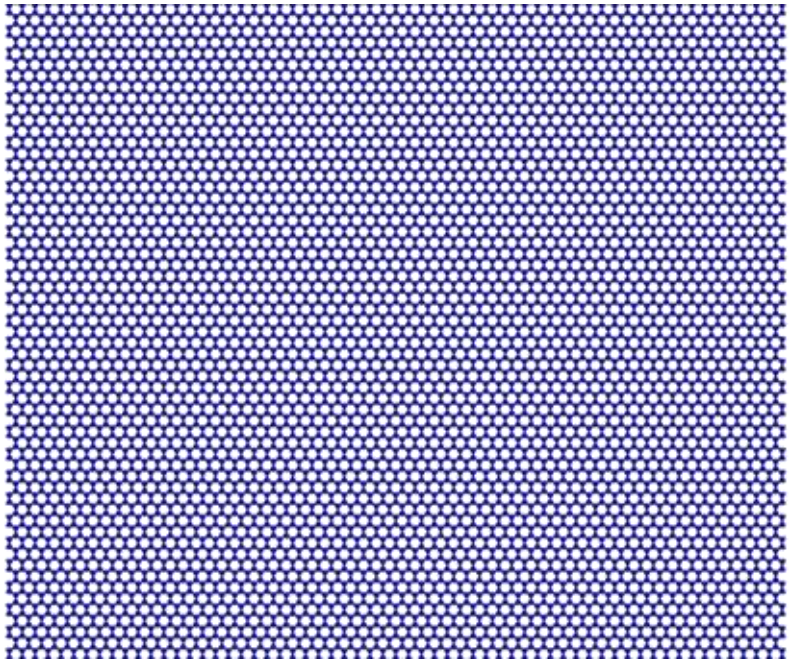

Record properties of graphene:

- Thinnest imaginable material → one atom thick
- Highest surface area → 2630 m^2/g
- Transparent to light → 97.7 %
- Ultra-broadband absorption → uV - THz
- Stiffest material → 1 TPa
- Strongest material → 130GPa
- Most stretchable material → 20%
- Record thermal conductivity → 6000 W/mK
- Highest current density at RT → 10^6 > copper
- Highest intrinsic mobility → 100 > Si
- Lightest charge carrier → massless Dirac fermions
- Longest mean free path at room temp → microns
- Easily functionalized and process able
- Impervious to even He

Graphene 2D band structure:

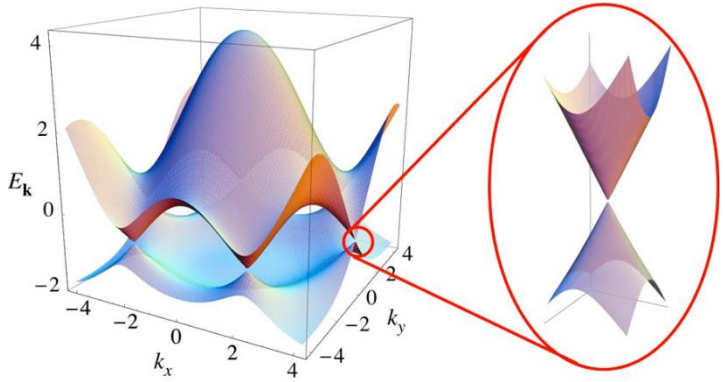

Dirac equation

$$\hat{H} = v_F \vec{\sigma} \cdot \hat{p}$$

Effective mass

$$m^* = \pm\hbar\left(\frac{\mathrm{d}^2 E_k}{\mathrm{d}k^2}\right)^{-1}$$

Graphene 2D Brillouin zone:

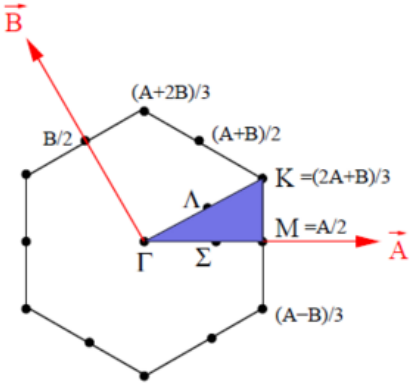

Graphene and 2D van der Waals materials

Graphene family	Graphene	hBN 'white graphene'	BCN	Fluorographene	Graphene oxide
2D chalcogenIdes	MoS_2, WS_2, $MoSe_2$, WSe_2	Semiconducting dichalcogenides: $MoTe_2$, WTe_2, ZrS_2, $ZrSe_2$ and so on		Metallic dichalcogenides: $NbSe_2$, NbS_2, TaS_2, TiS_2, $NiSe_2$ and so on	
				Layered semiconductors: GaSe, GaTe, InSe, Bi_2Se_3 and so on	
2D oxides	Micas, BSCCO	MoO_3, WO_3	Perovskite-type: $LaNb_2O_7$, $(Ca,Sr)_2Nb_3O_{10}$, $Bi_4Ti_3O_{12}$, $Ca_2Ta_2TiO_{10}$ and so on	Hydroxides: $Ni(OH)_2$, $Eu(OH)_2$ and so on	
	Layered Cu oxides	TiO_2, MnO_2, V_2O_5, TaO_3, RuO_2 and so on		Others	

A. Geim, et. al. Nature (2013).

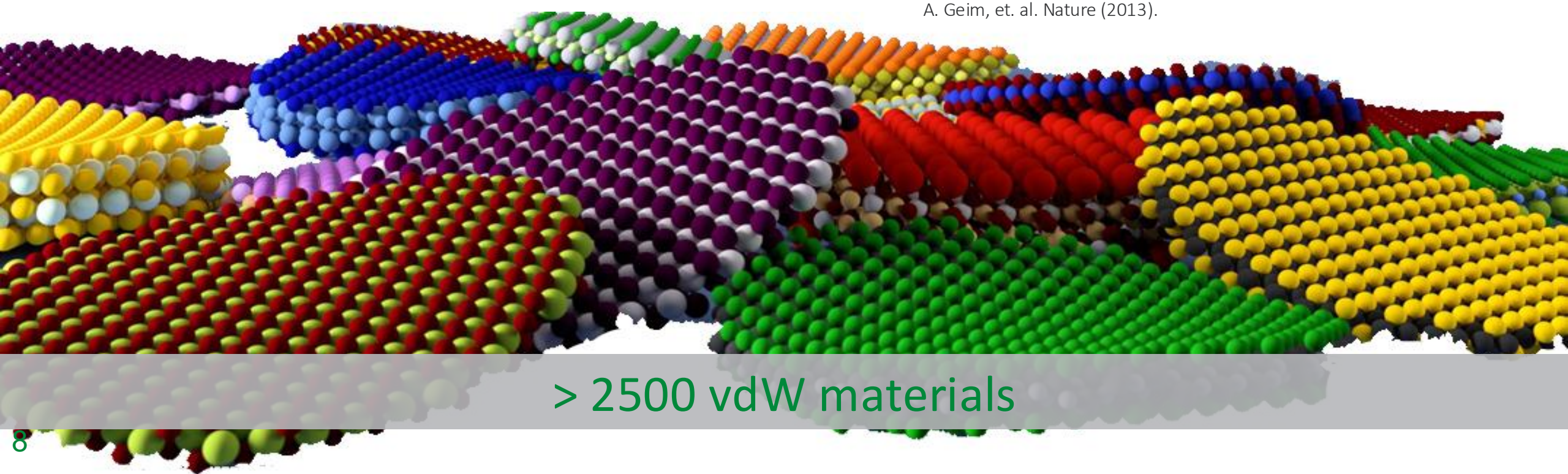

> 2500 vdW materials

VdW heterostructures – clean coupling over < 1nm

Efetov Lab

vdW co-lamination transfer technique:

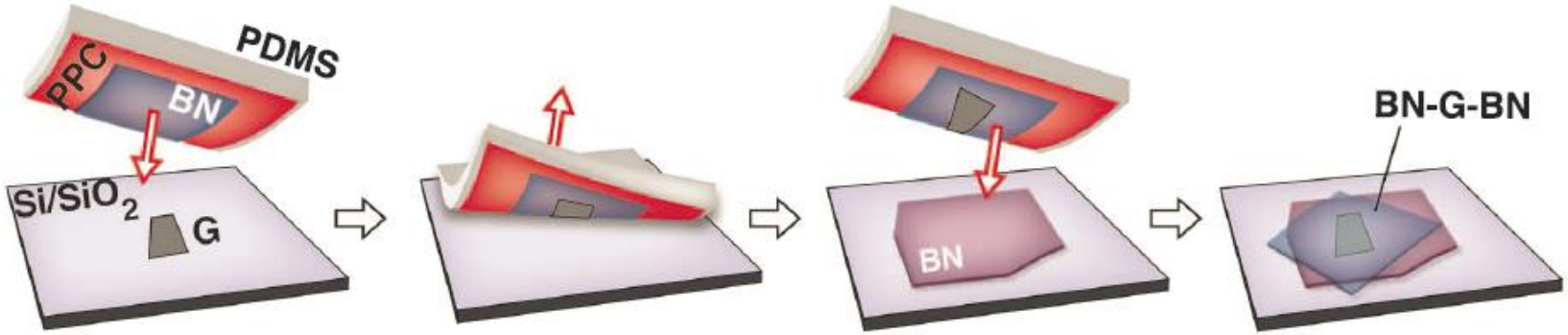

A. Geim, et. al. Nature (2013).

C.Dean, P. Kim, J. Hone, et. al. Science (2013).

Designer vdW stack:

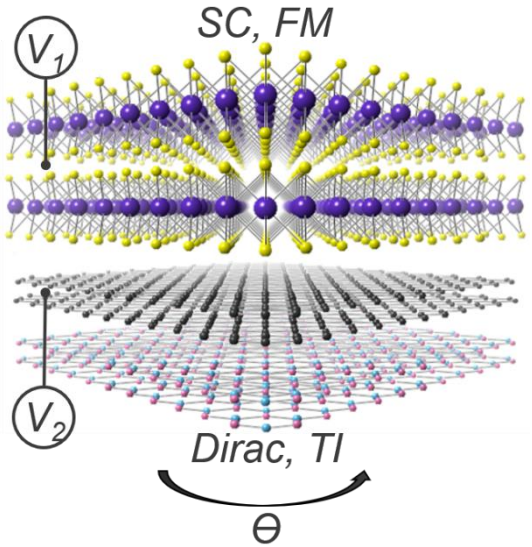

TEM cross-section:

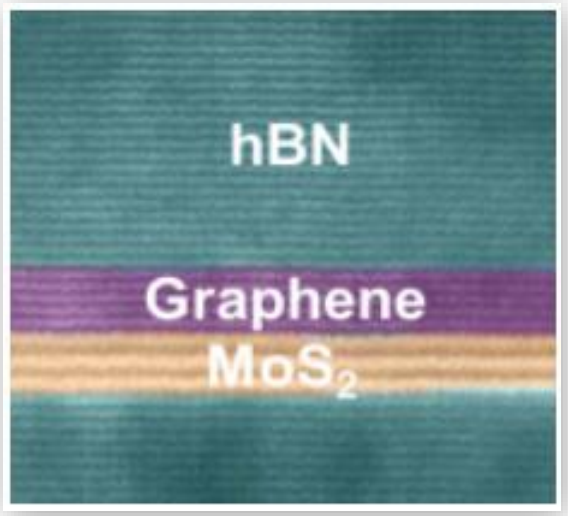

Moiré superlattice:

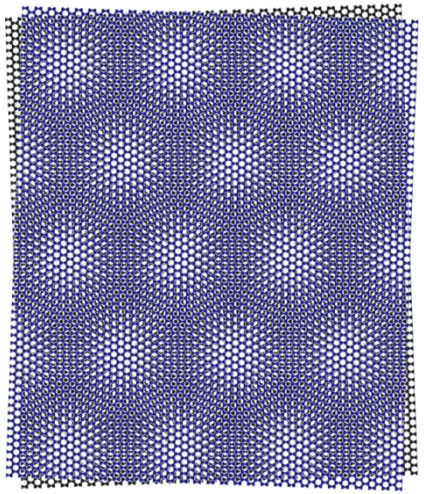

MBE (LEGO) vs. vdW (CARDS)

Efetov Lab

Molecular beam epitaxy:

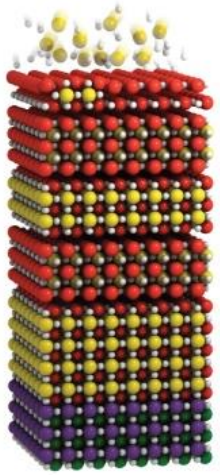

Van der Waals assembly:

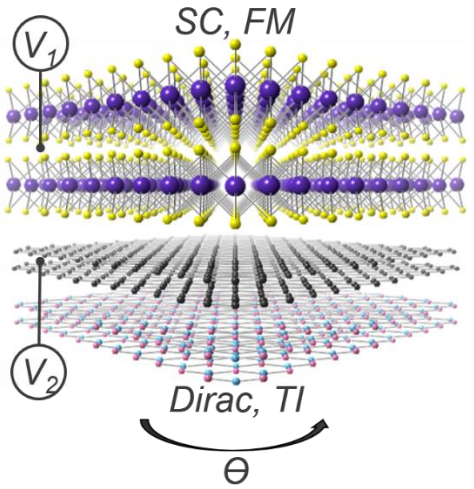

LEGO

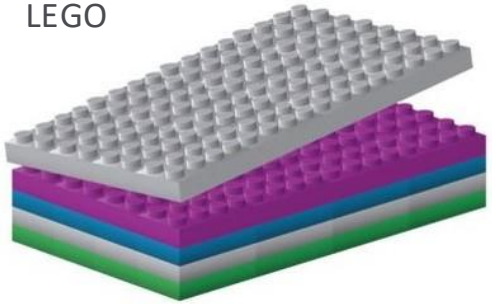

Crystallographic orientation locked

CARDS

Crystallographic orientation free

MBE (LEGO) vs. vdW (CARDS)

Molecular beam epitaxy:

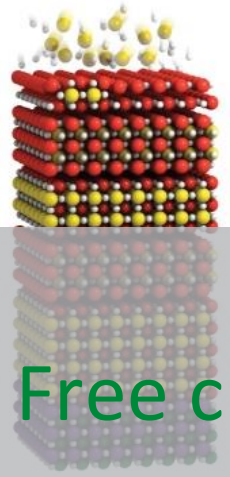

Van der Waals assembly:

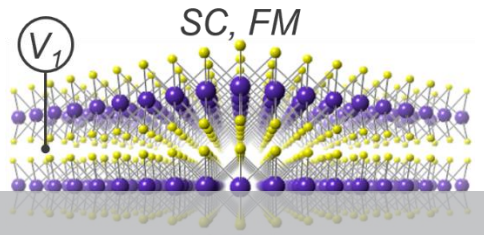

New → Free crystallographic orientation

LEGO

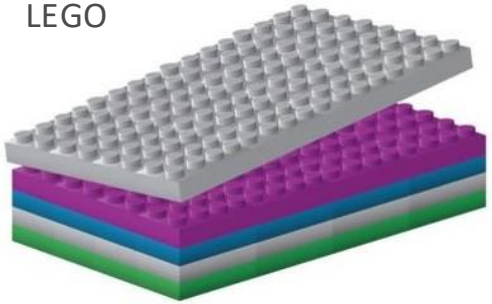

Crystallographic orientation locked

CARDS

Crystallographic orientation free

Moiré super-potential in twisted bilayer graphene

Twisted bilayer graphene:

Graphene cell, a ~ 0.14 nm

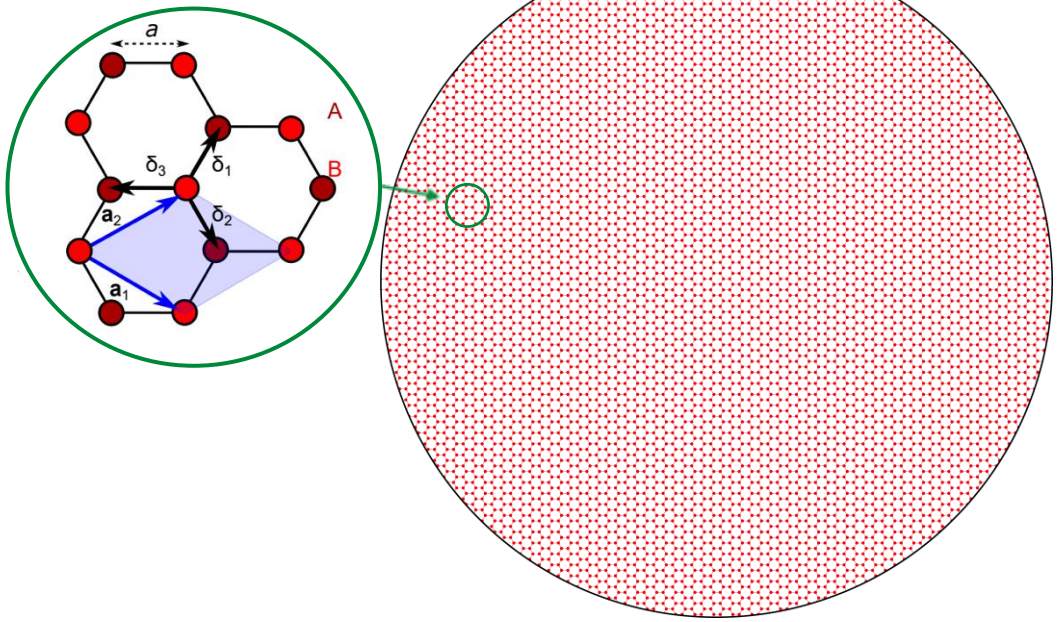

Single layer graphene:

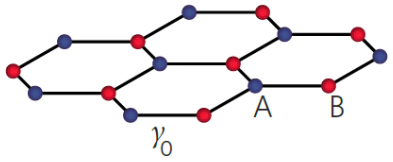

$$\varepsilon_{\pm}(\vec{k}) = \pm\gamma_0\sqrt{3+4\cos\left(\frac{\sqrt{3}ak_x}{2}\right)\cos\left(\frac{ak_y}{2}\right)+2\cos(ak_y)}.$$

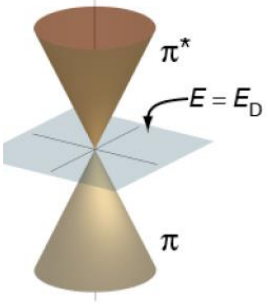

Moiré super-potential in twisted bilayer graphene

Efetov Lab

Twisted bilayer graphene:

Graphene cell, a ~ 0.14 nm

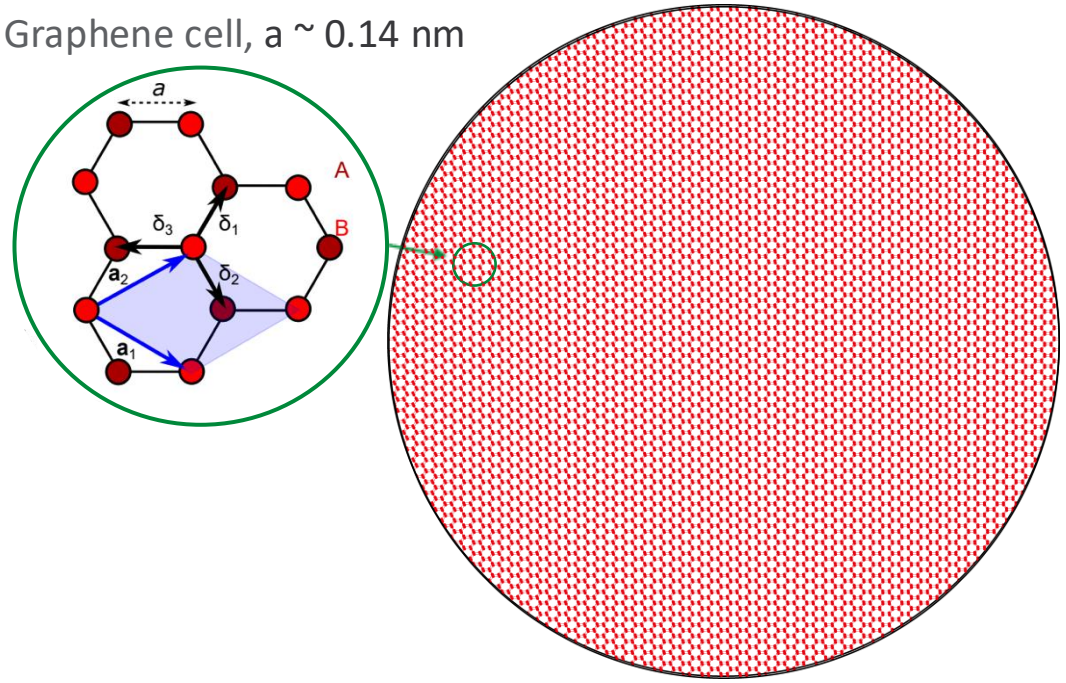

Single layer graphene:

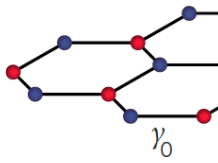

$$\varepsilon_{\pm}(\vec{k}) = \pm\gamma_0\sqrt{3+4\cos\left(\frac{\sqrt{3}ak_x}{2}\right)\cos\left(\frac{ak_y}{2}\right)+2\cos(ak_y)}.$$

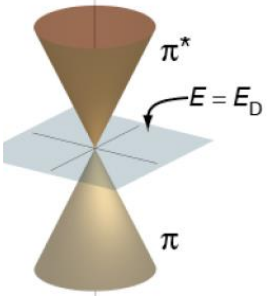

AB bilayer graphene:

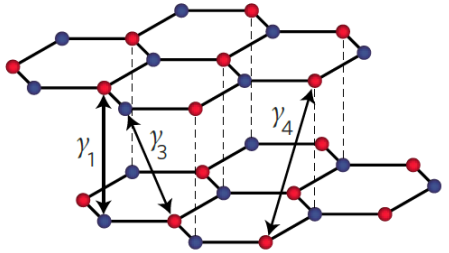

$$\varepsilon(p)^2 = (v_f p)^2 + \frac{\gamma_1^2}{2} + \frac{\Delta^2}{4} \pm \sqrt{(v_f p)^2(\gamma_1^2+\Delta^2)+\frac{\gamma_1^4}{4}}$$

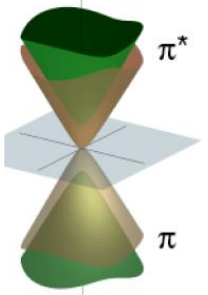

Moiré super-potential in twisted bilayer graphene

Twisted bilayer graphene:

Moiré Supercell,
λ ~ 10 nm

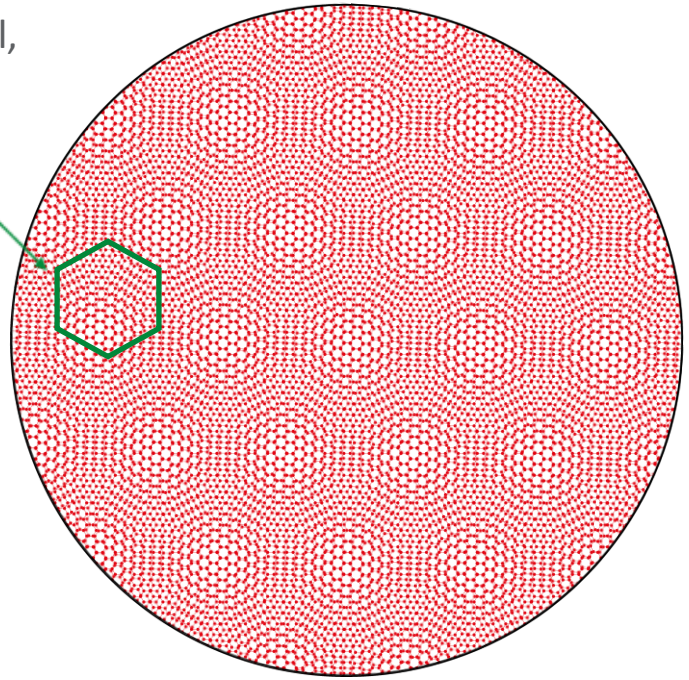

Single layer graphene:

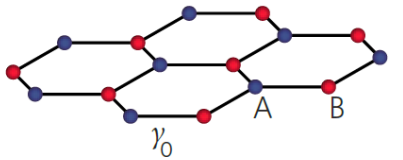

$$\varepsilon_{\pm}(\vec{k}) = \pm\gamma_0\sqrt{3+4\cos\left(\frac{\sqrt{3}ak_x}{2}\right)\cos\left(\frac{ak_y}{2}\right)+2\cos(ak_y)}.$$

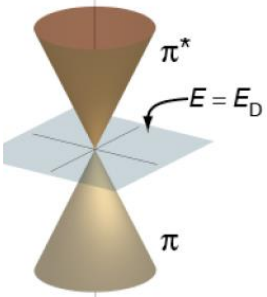

AB bilayer graphene:

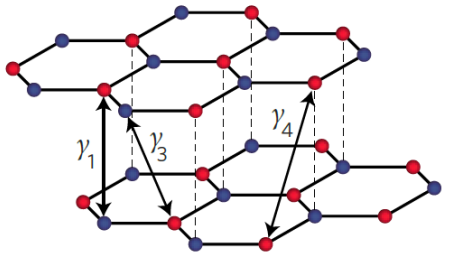

$$\varepsilon(p)^2 = (v_f p)^2 + \frac{\gamma_1^2}{2} + \frac{\Delta^2}{4} \pm \sqrt{(v_f p)^2(\gamma_1^2+\Delta^2)+\frac{\gamma_1^4}{4}}$$

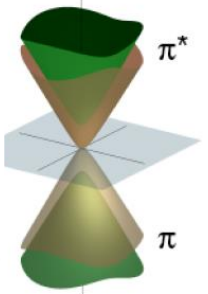

Atomic arrangement:

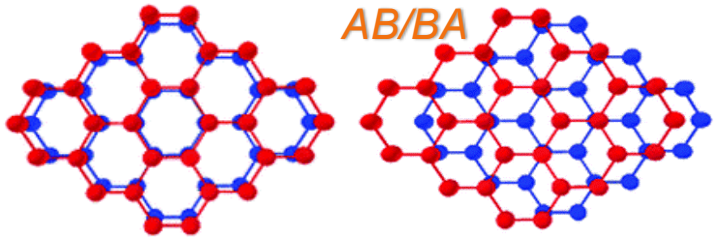

Height profile:

Brillouin zone:

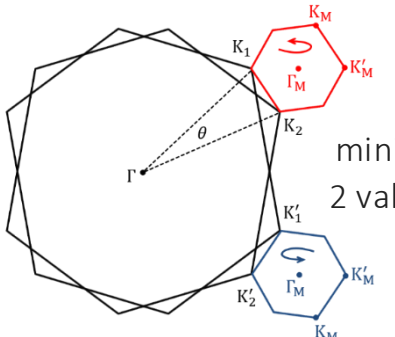

mini-BZ
2 valleys

Bistritzer-MacDonald continuum model & the magic angle

Twisted bilayer graphene:

Moiré Supercell,
λ ~ 10 nm

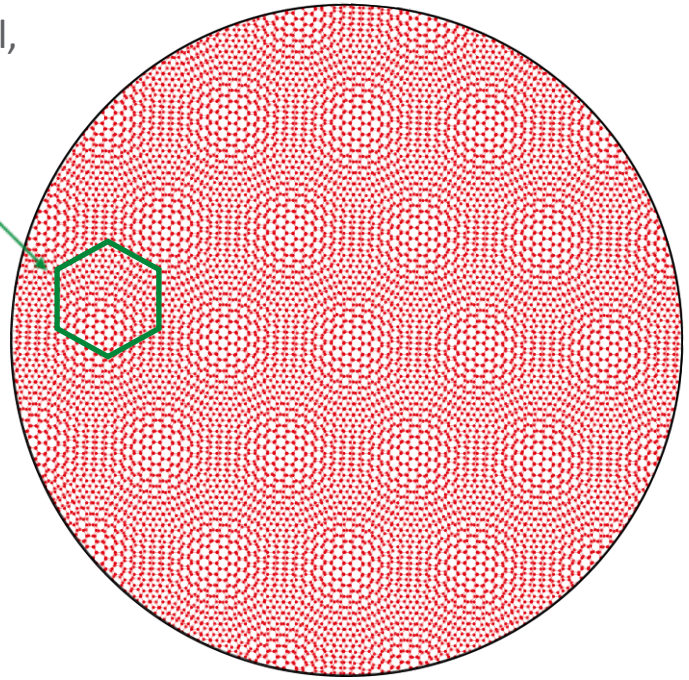

Bistritzer R. and MacDonald A.H., PNAS, **108,** (2011)

$$H_K = \begin{pmatrix} v_F \boldsymbol{\sigma} \cdot \boldsymbol{p}_1 & T(\boldsymbol{r}) \\ T^\dagger(\boldsymbol{r}) & v_F \boldsymbol{\sigma} \cdot \boldsymbol{p}_2 \end{pmatrix}$$

$$T(\boldsymbol{r}) = \sum_{n=0}^{2} T_{n+1} e^{-i\boldsymbol{q}_{n+1}\boldsymbol{r}}$$

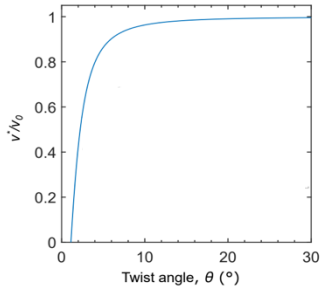

Band-structure vs. θ in TBG:

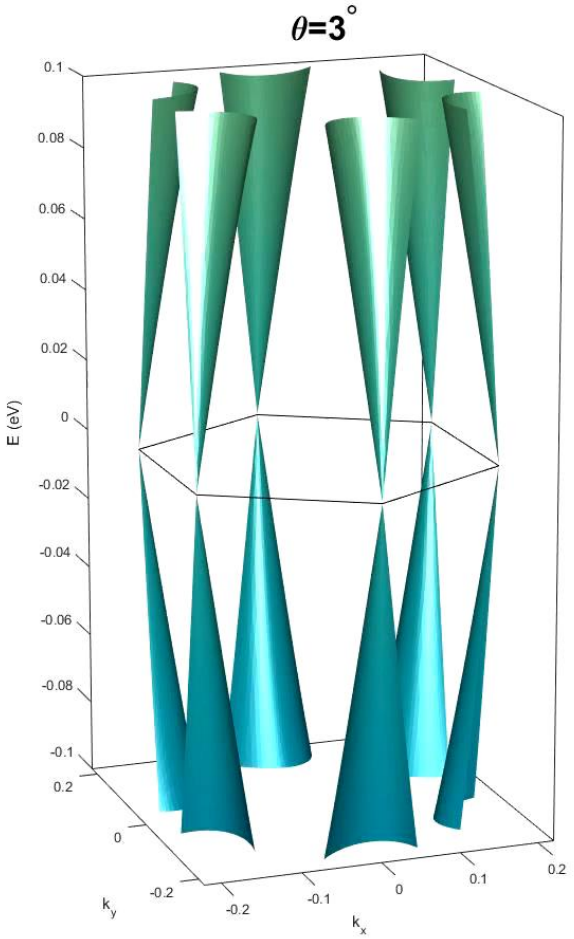

Cao Y. et al., Nature **556**, 80 (2018)

Topological flat-bands in MATBG

Spin/valley degenerate flat bands:

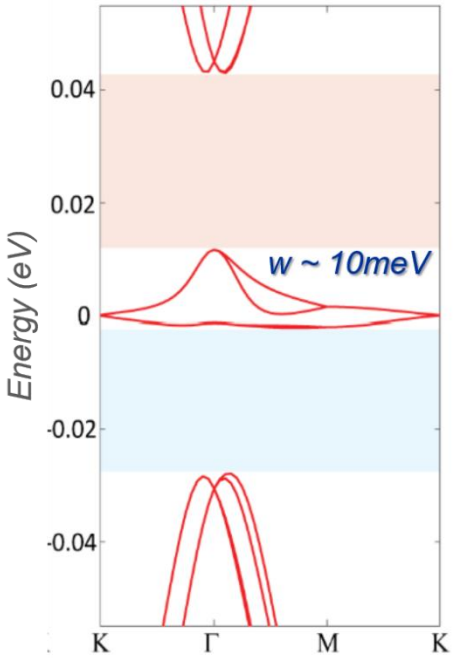

Continuum model calculations
(Bistritzer/MacDonald) + corrugations/strain

H. Yoo, … , E. Kaxiras, P. Kim, Nature Materials 18, 448 (2019).

and many many others.

Berry curvature in mini-BZs add up:

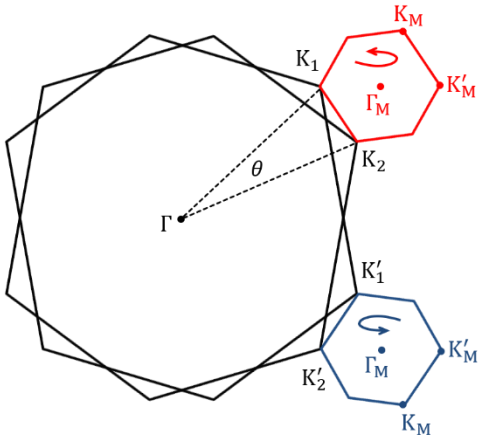

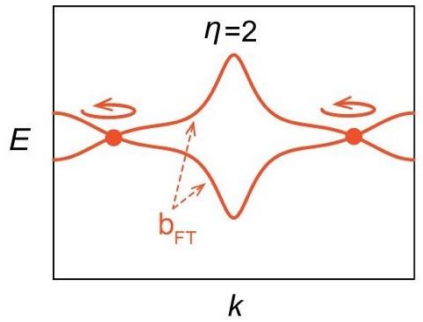

- Spin/valley degeneracy 4e/uc
- Mini-BZs decoupled
- No localized Wannier functions → Chern bands
- Interactions can break C_2T symmetries

Bernevig group (2018).
MacDonald group (2019).
Fu group (2018).
Vishnawanth group (2018).
Zaletel group (2018).
Todadri group (2019).

Topological flat-bands in MATBG

Spin/valley degenerate flat bands:

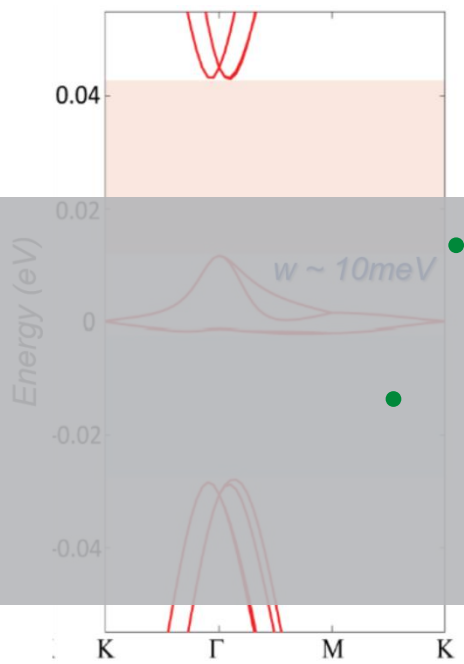

Continuum model calculations
(Bistritzer/MacDonald) + corrugations/strain

H. Yoo, … , E. Kaxiras, P. Kim, Nature Materials 18, 448 (2019).

and many many others.

Berry curvature in mini-BZs add up:

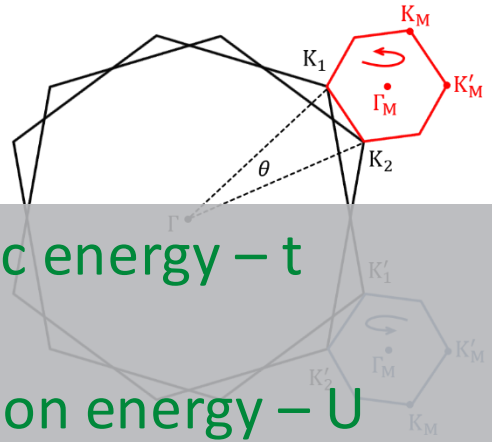

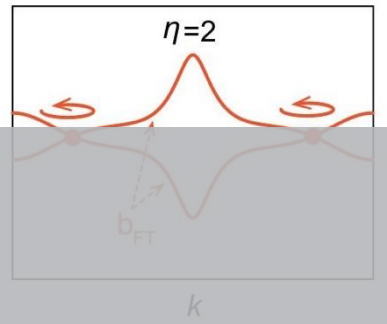

- quenched kinetic energy – t
- dominant interaction energy – U
- bands are topological

- Spin/valley degeneracy 4e/uc
- mini-BZs decoupled
- No localized Wannier functions → Chern bands
- Interactions can break C_2T symmetries

Bernevig group (2018).
MacDonald group (2019).
Fu group (2018).
Vishnawanth group (2018).
Zaletel group (2018).
Todadri group (2019).

High-quality assembly of next generation moiré materials

Efetov Lab

Torsional force microscopy (TFM):

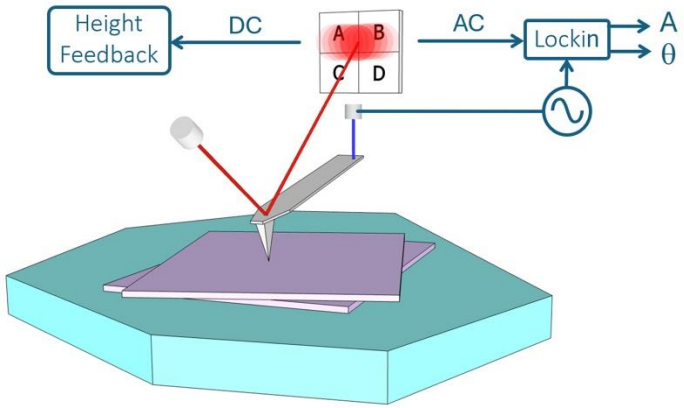

Pendharkar, M., PNAS 10 (2024).

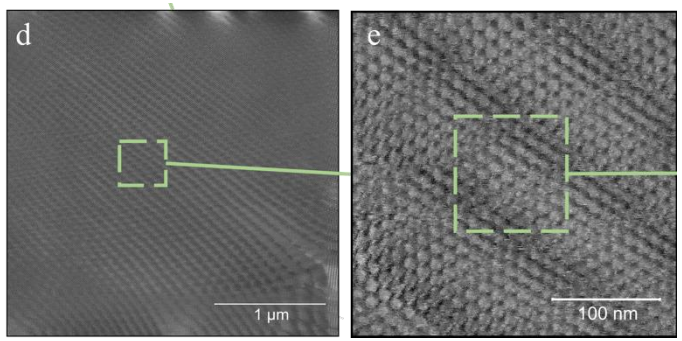

Scanning Microwave Impedance Microscopy (sMIM):

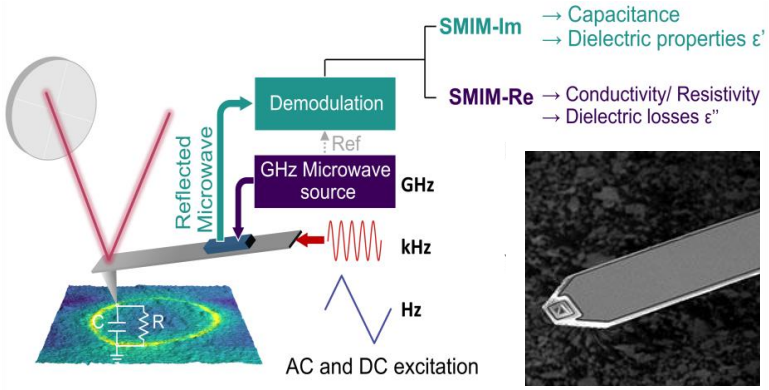

Bargas G., Phys. Stat. Sol. B, (2024).

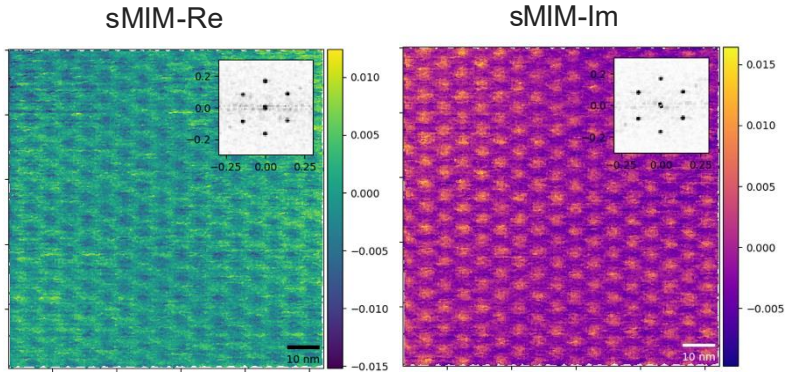

Deterministic edge clamping and bubble removal:

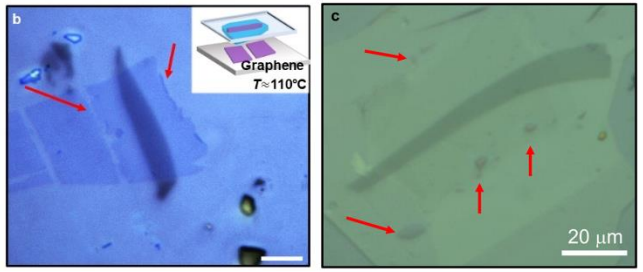

Optimized device design:

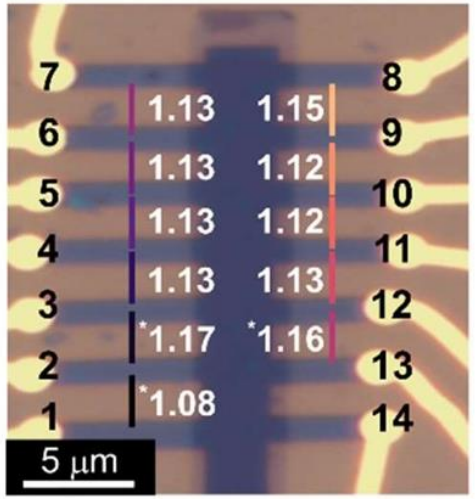

- Production of ultra-homogeneous MATBG devices.
- Production of MATBG devices with well defined strain profiles.
- Twist angle variation $\Delta\theta \leq 0.02°$, with homogenous regions up to ~ 36 μm^2.

J. Diez, … , DKE, **Newton, 1, 100007 (2025).**

Moiré super-lattice and flat bands in tBLG

Efetov Lab

STM - Moiré topography:

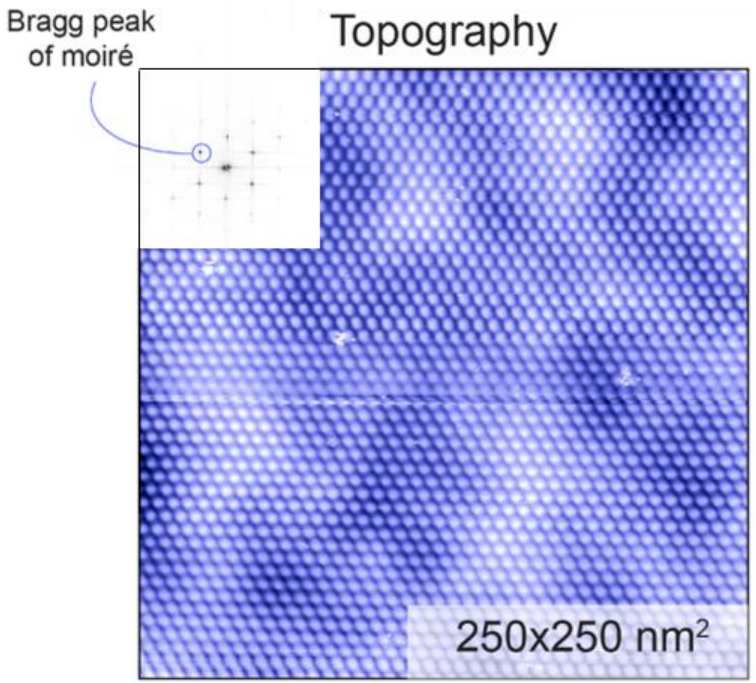

T. Benshop, … , DKE, M. Allan, PRR 3, 013153 (2021).

Nadj-Perge group, Nature Physics (2019).
Yazdani group, Nature (2019).
Pasupathy group, Nature (2019).
Andrei group, Nature (2019).

Nano-ARPES for θ ~ 1.3˚:

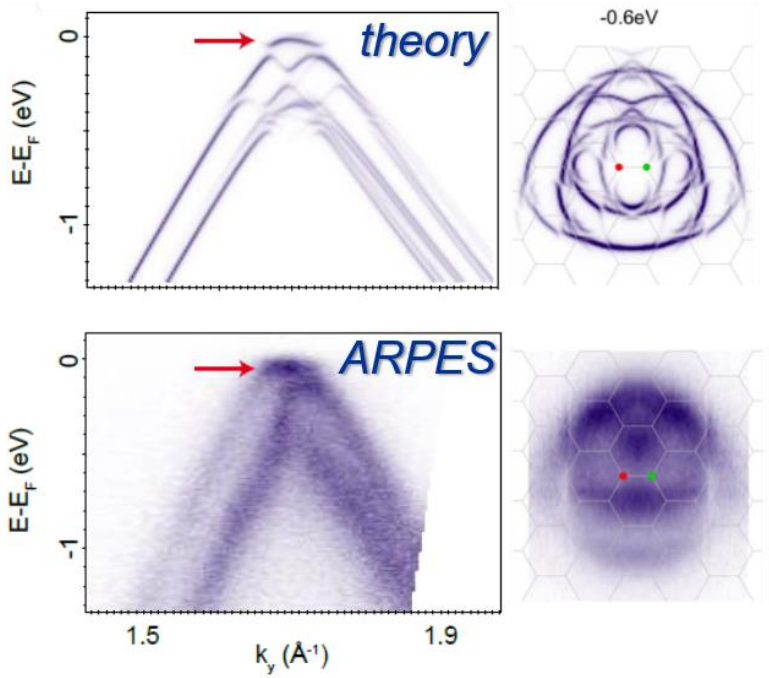

S. Lisi, … , DKE, F. Baumberger, Nature Physics 17, 189 (2021).

Also:

M. Utama, ... , F. Wang, Nature Physics (2020).

Transport Measurements

Device Structure:

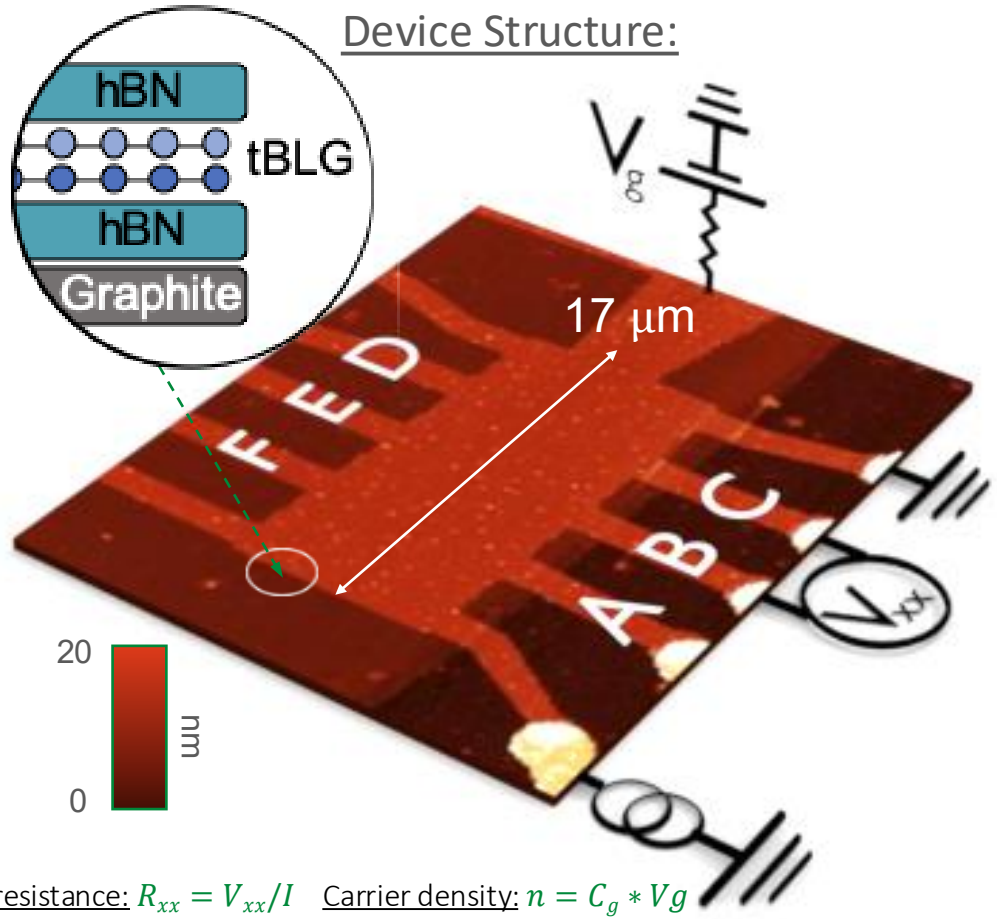

Tuning Fermi Energy:

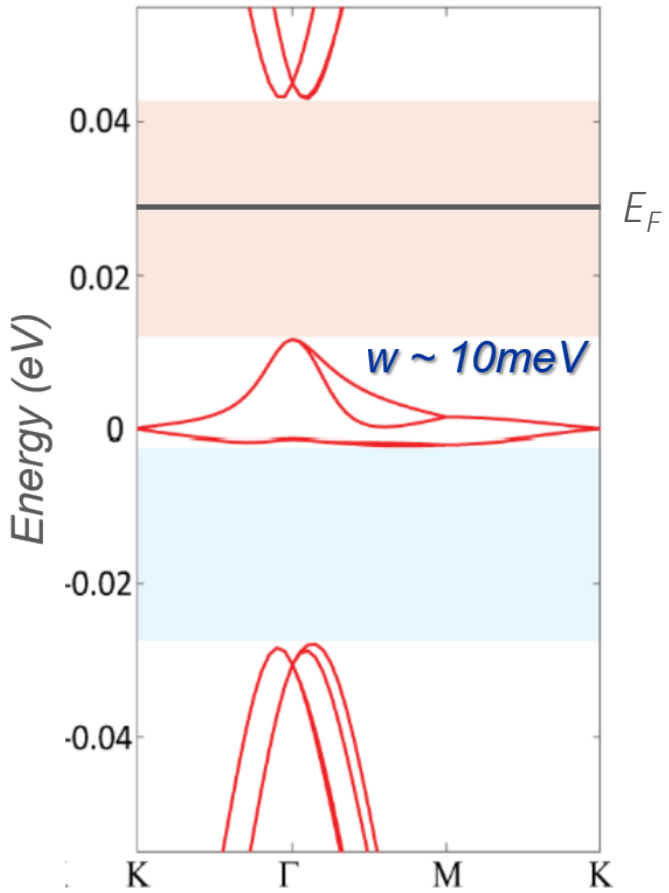

Longitudinal resistance: $R_{xx} = V_{xx}/I$ Carrier density: $n = C_g * Vg$

Hall resistance: $R_{xy} = V_{xy}/I$ Hall density: $n = n_H = -B/eR_{xy}$

MATBG – temperature and filling dependent phase diagram

Superconductivity:

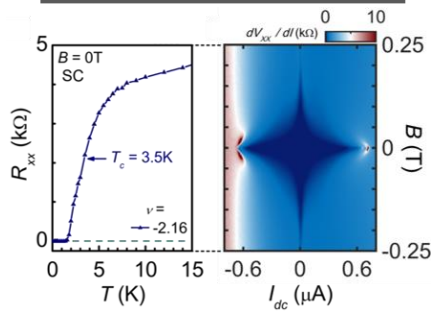

P. Stepanov, I. Das, X.Lu, … , DKE, Nature 583, 375 (2020).

CI: correlated insulator, SC: superconductor, PM: Pomeranchuk-effect, SM: strange metal,
FL: Fermi liquid, CCI: Correlated Chern insulator, C: Chern number

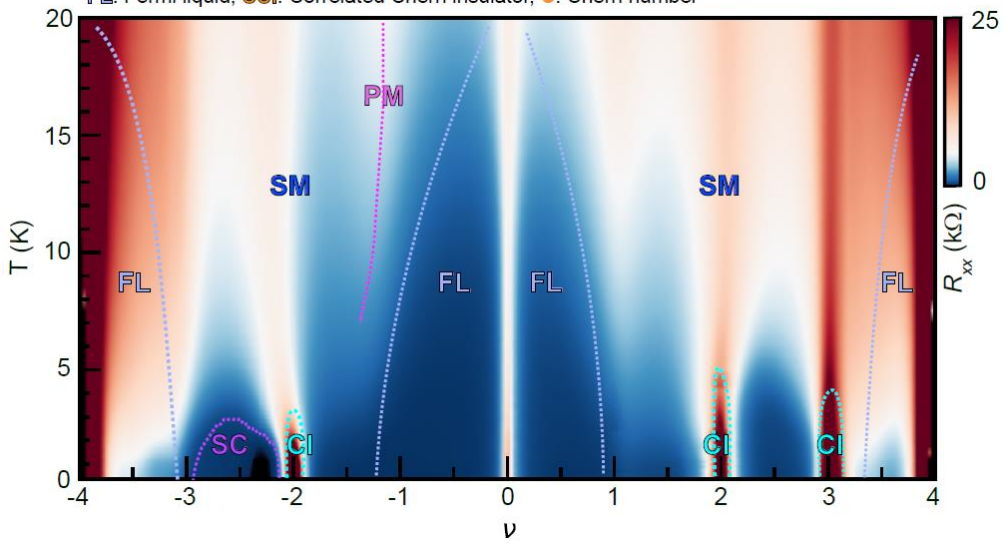

Correlated Insulators:

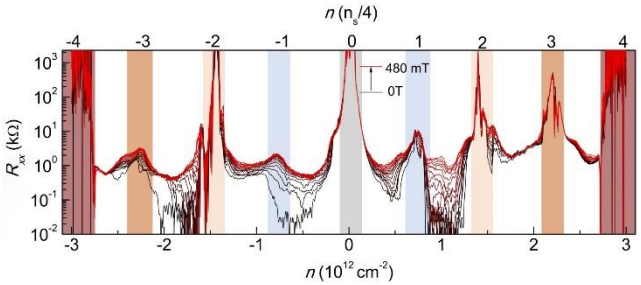

X. Lu, … , DKE, Nature 574, 653 (2019).

Strange metal:

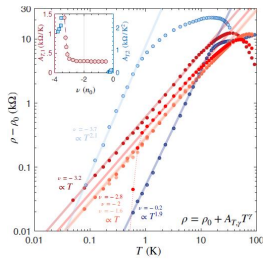

A. Jaoui, … , DKE, Nature Physics 18, 633 (2022).

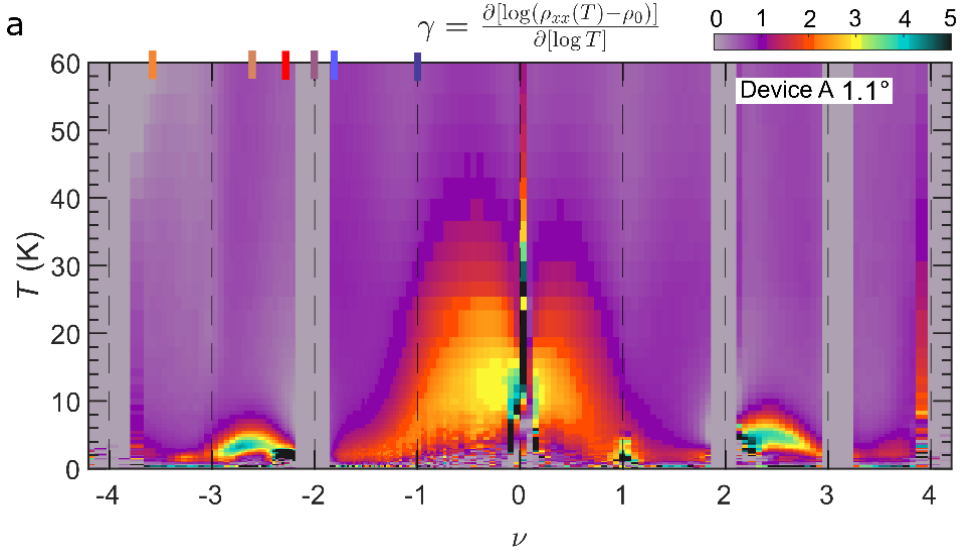

Pomeranchuk effect:

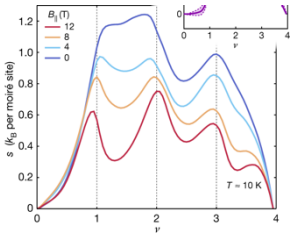

A. Rozen, … , S. Ilani, Nature 592, 214 (2021).

Topological heavy fermion model (THF)

Efetov Lab

BM model:

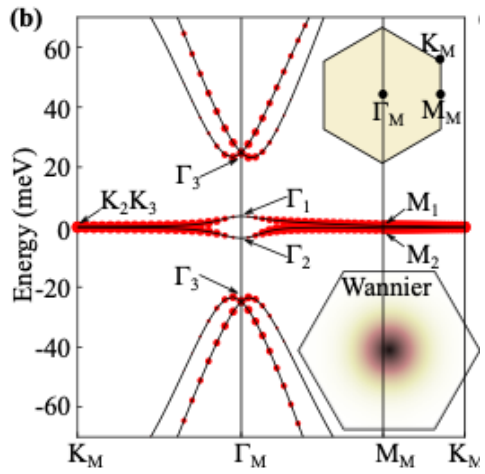

- Flat-band regions host slow and heavy electrons.
- Dispersive band regions prevail in the Γ-point due to topological obstruction.

Mapping of BM onto THF model:

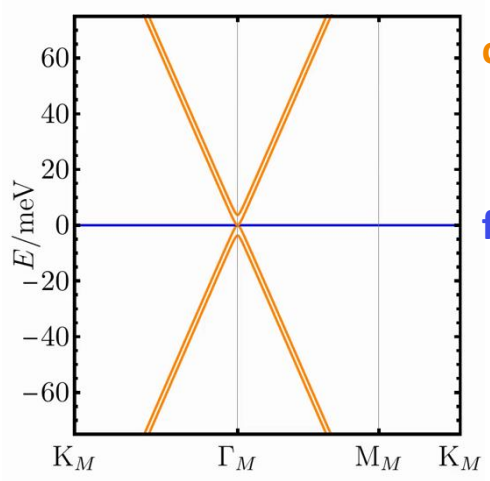

- Basis transformation allows to decompose flat-band regions (f-bands) and dispersive band regions (c-bands).
- Hybridisation of f and c bands leads to a direct mapping onto the BM model.

THF picture:

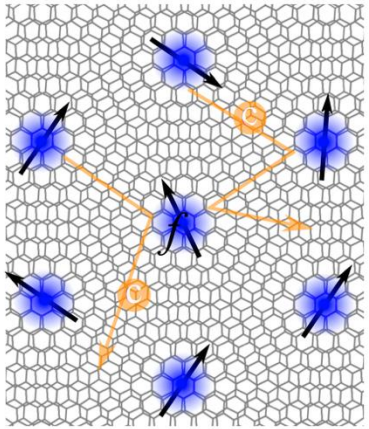

- Lattice of strongly-interacting, localized (heavy) **f-electrons** → carry flatness.
- Nearly-free background of itinerant (light) **c-electrons** → carry topology.

→ Direct mapping of BM onto the THF model.
→ Localized f- and topological c-bands.
→ DMFT calculations possible.

Z.D. Song et. al. PRL 103, 205414 (2022).

Also: Bascones, Berg, Kalaf, Vishnavanth, Glazman, Valenti, Wehling, SanGiovanni

Mott phase of topological bands in THF picture

Effective Hamiltonian Including Coulomb and Exchange:

$$\hat{H}_{THF} = \hat{H}_0 + \hat{H}_U + \hat{H}_V + \hat{H}_W + \hat{H}_J$$

$H_U = \frac{U}{2}\sum \hat{f}^\dagger \hat{f} \hat{f}^\dagger \hat{f}$

Coulomb repulsion between f

$U \sim 60$ meV

$H_V = V \sum \hat{c}^\dagger \hat{c} \hat{c}^\dagger \hat{c}$

Coulomb repulsion between c

$V \sim 40$ meV

$H_W = W \sum \hat{c}^\dagger \hat{c} \hat{f}^\dagger \hat{f}$

Coulomb repulsion between c and f

$W \sim 40$ meV

$H_J = -J \sum S_f S_c$

Exchange between c and f electrons

$J \sim 15$ meV

Unhybridized spectral function at ν = 0 (including U):

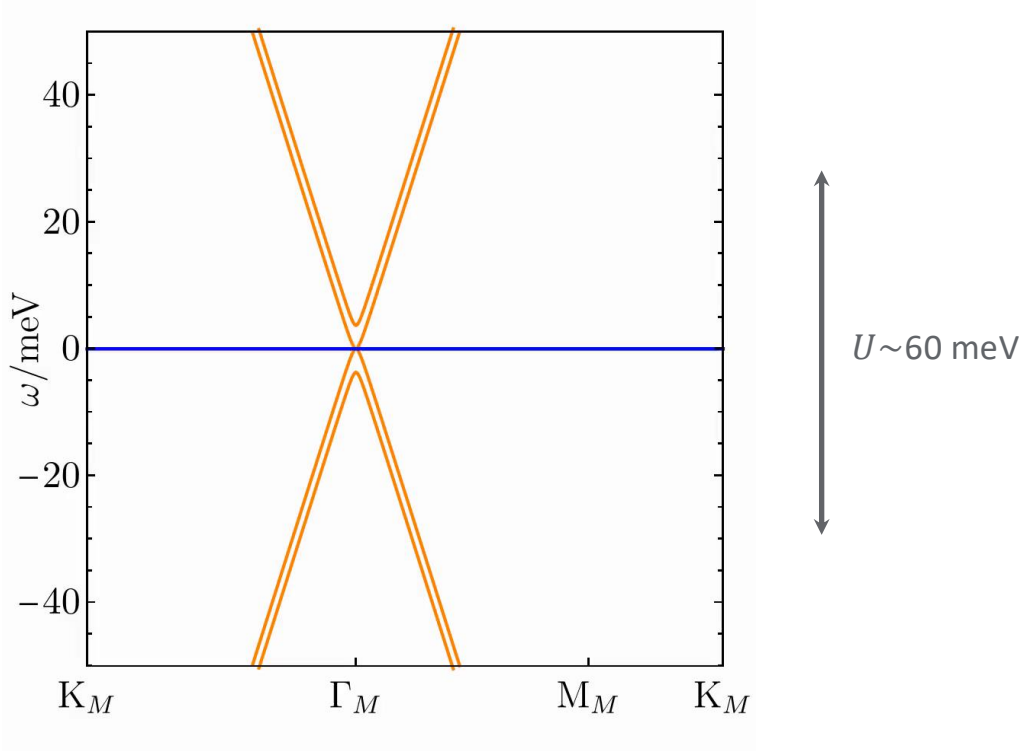

Mott phase of topological bands in THF picture

Effective Hamiltonian Including Coulomb and Exchange:

$$\hat{H}_{THF} = \hat{H}_0 + \hat{H}_U + \hat{H}_V + \hat{H}_W + \hat{H}_J$$

$H_U = \frac{U}{2}\sum \hat{f}^\dagger \hat{f} \hat{f}^\dagger \hat{f}$
Coulomb repulsion between f
U~60 meV

$H_V = V\sum \hat{c}^\dagger \hat{c} \hat{c}^\dagger \hat{c}$
Coulomb repulsion between c
V~40 meV

$H_W = W\sum \hat{c}^\dagger \hat{c} \hat{f}^\dagger \hat{f}$
Coulomb repulsion between c and f
W~40 meV

$H_J = -J\sum S_f S_c$
Exchange between c and f electrons
J~15 meV

Hybridized DMFT spectral function at ν = 0 (including U):

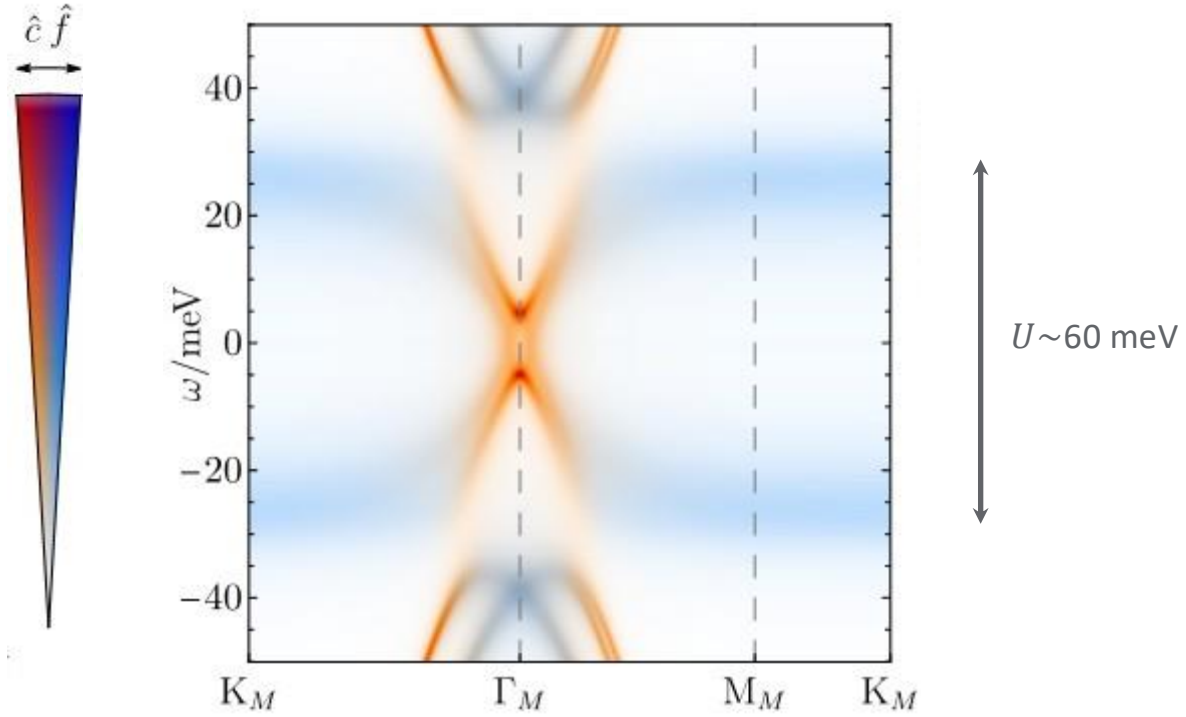

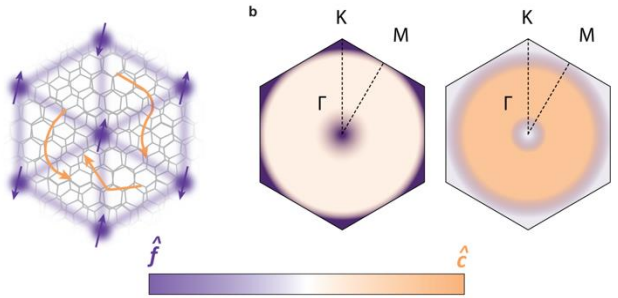

$\Sigma(w)$ → $\mathbb{R}[\Sigma(w)]$ Energy of quasiparticle

$\Sigma(w)$ → $\mathbb{I}[\Sigma(w)]$ Lifetime of quasiparticle

→ DMFT provides energy and lifetime of quasi-particles.

J. Xiao, et al., arXiv:2506.20738 (2025).
D. Călugăru, et al., arXiv:2509.18256 (2025).

Mott phase of topological bands in THF picture

Efetov Lab

f-electrons produce:
→ Spectrally broadened Hubbard bands
→ Fluctuating local moments

c-electrons produce:
→ Gapless – Mott semimetal.

Interaction between c and f:
→ Scatter efficiently
→ Kondo interaction

→ Not yet including ordering of f through J.

Hybridized DMFT spectral function at ν = 0 (including U):

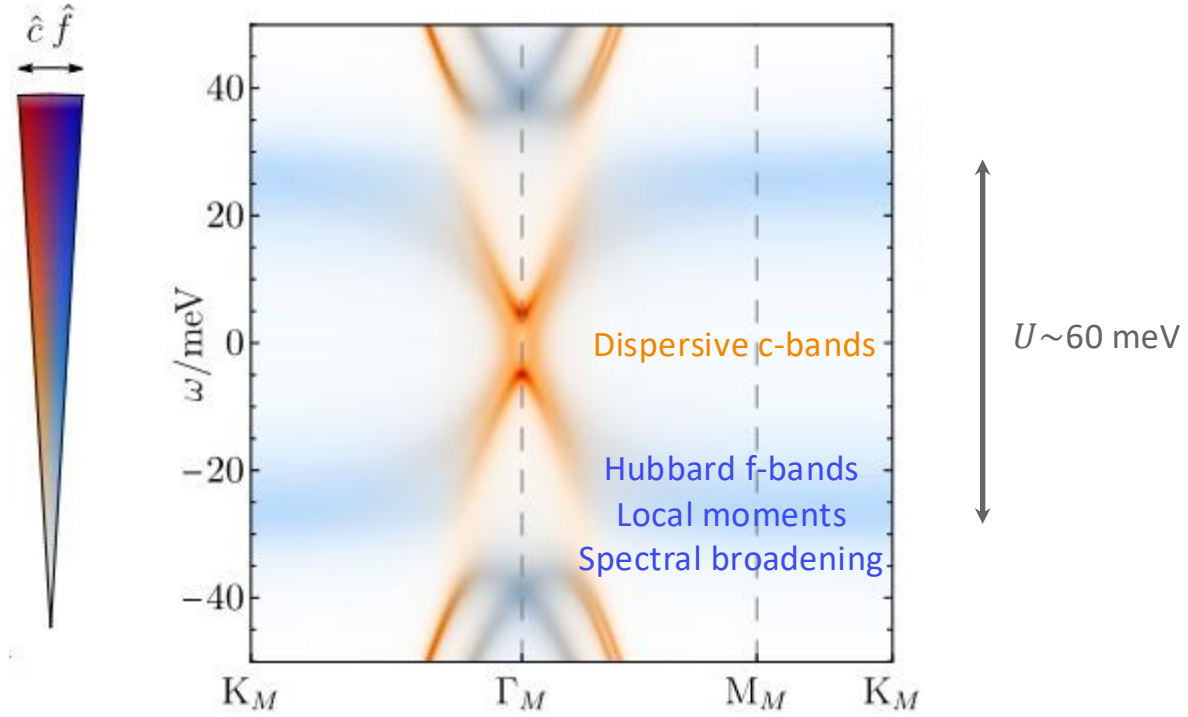

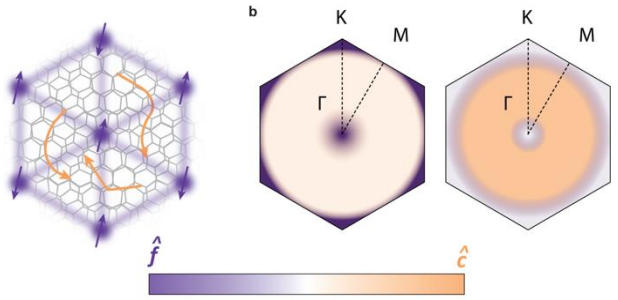

$\Sigma(w)$ → $\mathbb{R}[\Sigma(w)]$ Energy of quasiparticle
$\Sigma(w)$ → $\mathbb{I}[\Sigma(w)]$ Lifetime of quasiparticle

→ DMFT provides energy and lifetime of quasi-particles.

J. Xiao, et al., arXiv:2506.20738 (2025).
D. Călugăru, et al., arXiv:2509.18256 (2025).

Mott phase of topological bands & topological Kondo lattice

Kondo bands from hybridized f and c:

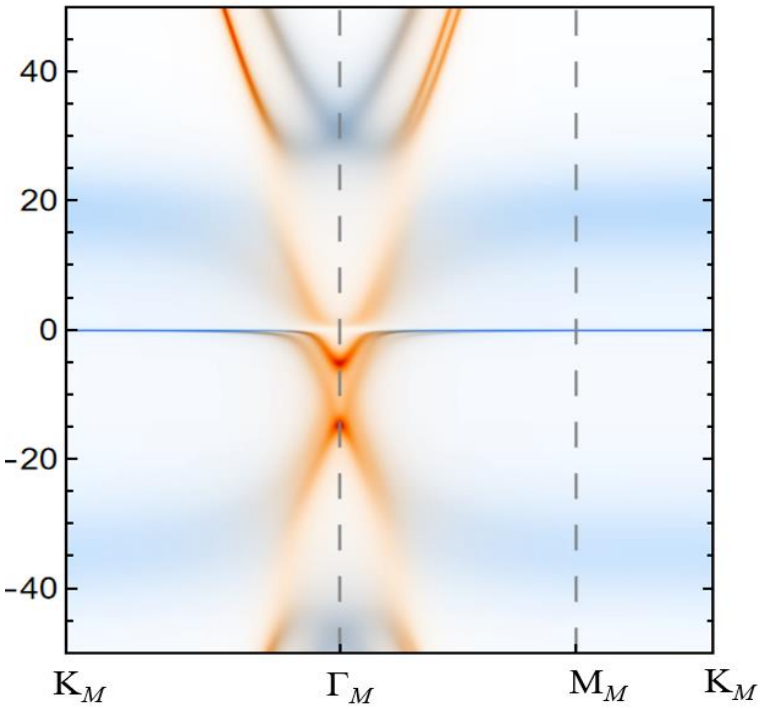

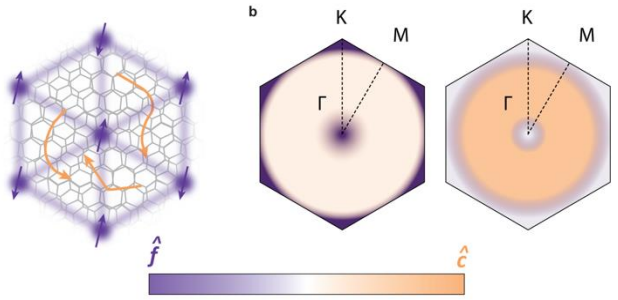

Ordering of f-electrons can increase coherence:

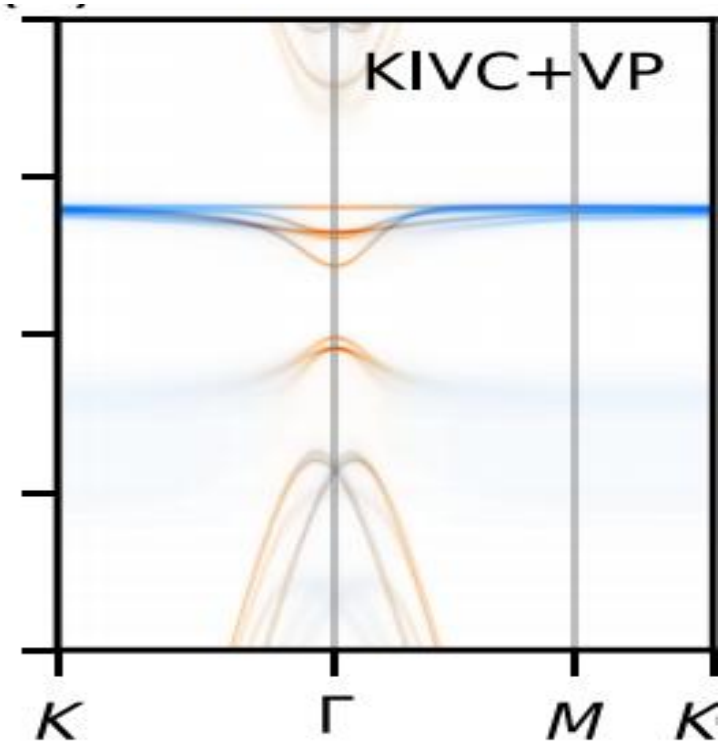

$\Sigma(w)$ → $\mathbb{R}[\Sigma(w)]$ Energy of quasiparticle

$\Sigma(w)$ → $\mathbb{I}[\Sigma(w)]$ Lifetime of quasiparticle

→ DMFT provides energy and lifetime of quasi-particles.

J. Xiao, et al., arXiv:2506.20738 (2025).
D. Călugăru, et al., arXiv:2509.18256 (2025).

Most reproducible MATBG phase diagram

Open questions?

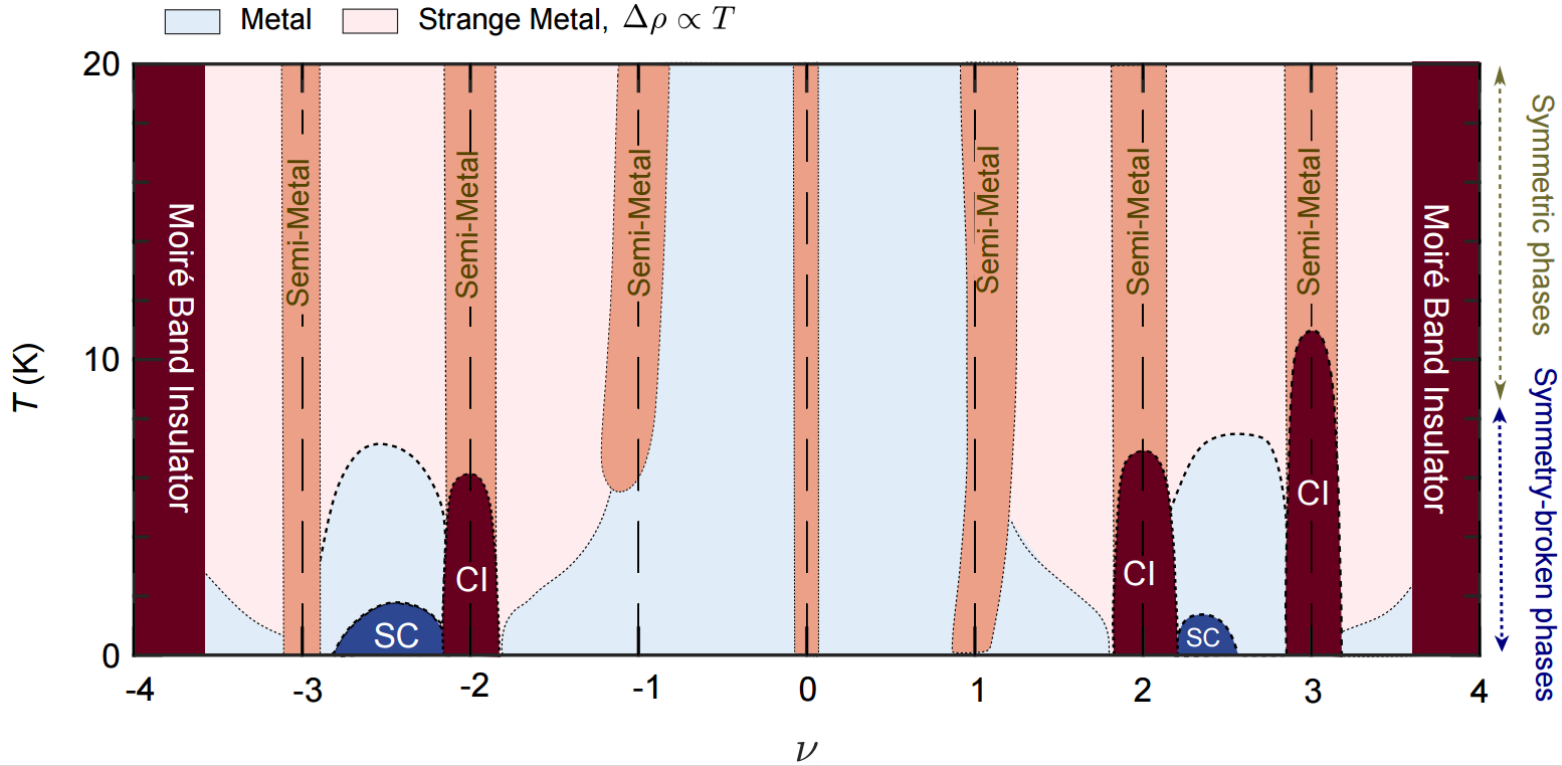

States at integer filling $\nu = 0, \pm 1, \pm 2, \pm 3$:

- T > 10K → all show semi-metallic resistance peaks.
- T < 10K → distinct behaviour of $\nu = -1, -2$ etc. Clear signatures of symmetry breaking set-in (Hall resets).

Superconductivity:

- By far most common and strongest for $\nu = -2 - \delta$ and less common for $\nu = 2 + \delta$. All other regions rare.

Metallic states:

- T > 10K → broad range of R ~ T strange metal.
- T < 10K → many region become good metals.
- New → between $\nu = \pm 2 - \pm 3$, a previously overlooked metallic dome, which can be associated with the pseudo-gap and IVC order. SC originates predominantly in this metallic state.

Magic angle twisted bilayer graphene - Phase diagram

Chern Insulators:

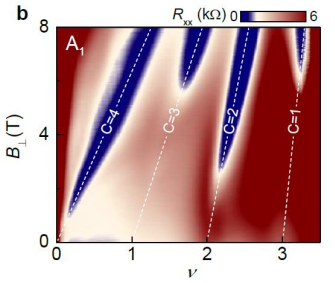

I. Das, X. Lu. … , DKE, Nature Physics 17, 710 (2021).

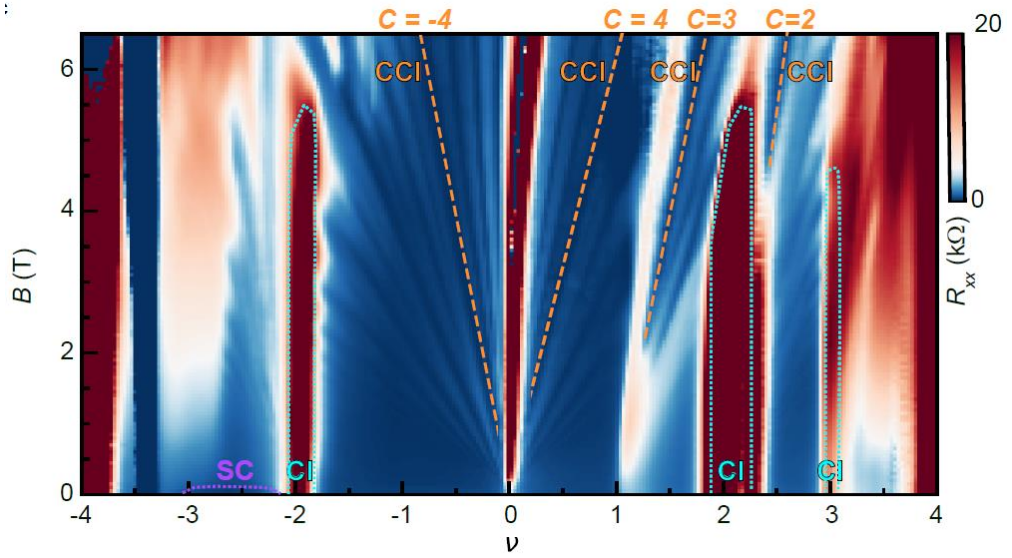

Orbital Magnetism:

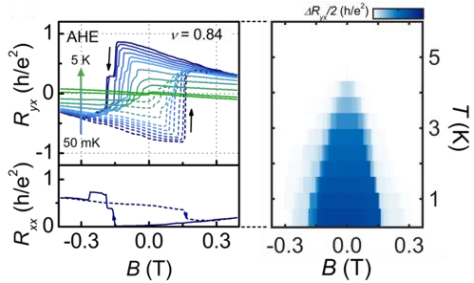

P. Stepanov, … , A. Bernevig, DKE, PRL 127, 197701 (2021).

Topological flat-bands in tBLG

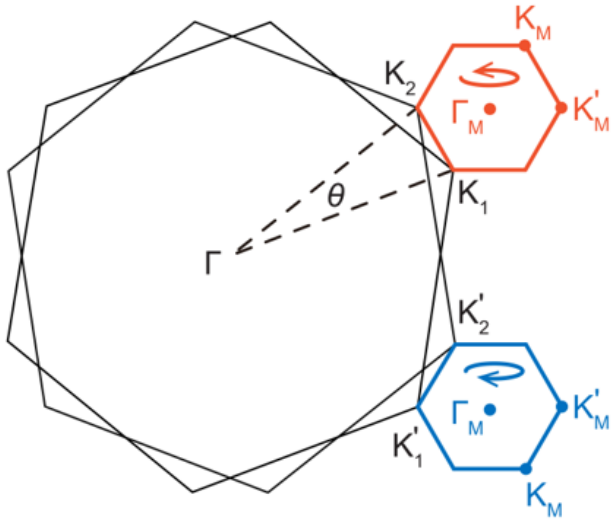

Mini-BZ with helicity $\eta = \pm 2$:

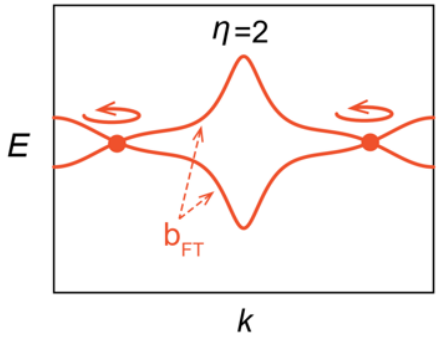

$$H_K \sim h v_F \boldsymbol{\sigma} \boldsymbol{k}$$

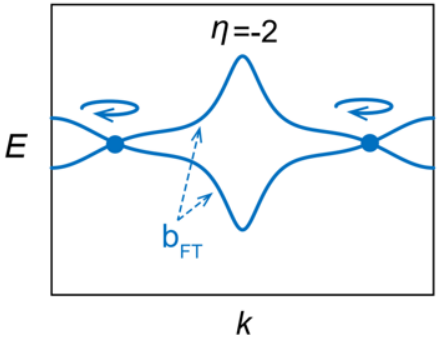

$$H_{K'} \sim -h v_F \boldsymbol{\sigma}^* \boldsymbol{k}$$

- Mini-BZs decoupled
- No localized Wannier functions → Chern bands
- C_2T - symmetry

Spin ↑,↓; Valley K, K'; Sublattice A, B;

- 4 Chern bands with C = -1
- 4 Chern bands with C = 1

Vafek group (2018).
Bernevig group (2018).
MacDonald group (2019).
Fu group (2018).

C = -1: | ↑, K', A>, | ↓, K', A>, | ↑, K, B>, | ↓, K, B>;

C = 1: | ↑, K, A>, | ↓, K, A>, | ↑, K', B>, | ↓, K', B>;

Vishnawanth group (2018).
Zaletel group (2018).
Todadri group (2019).
Dai group (2019).
Balents (2019).

Theoretical B-field phase diagram of MATBG

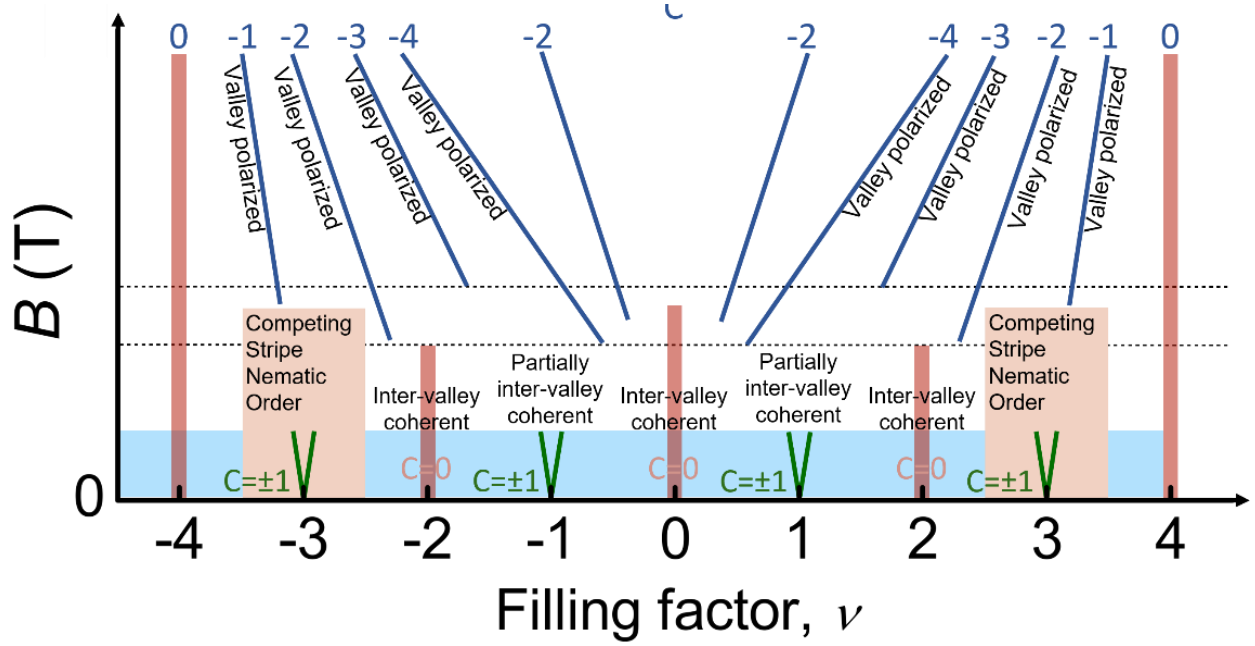

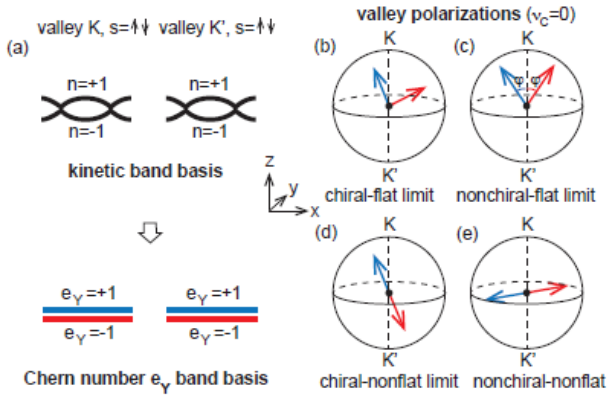

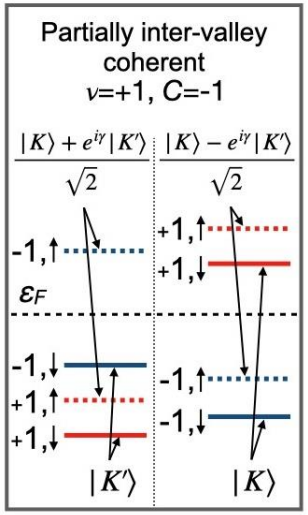

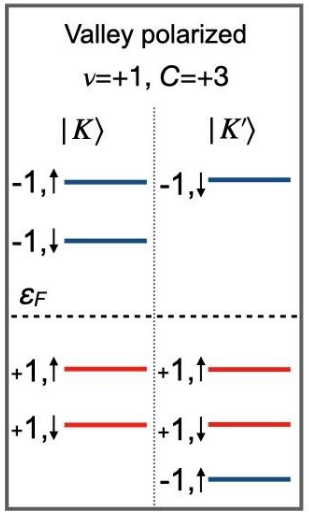

B. Lian, … ,B. A. Bernevig, PRB 103, 205414 (2021).
P. Stepanov, … , A. Bernevig, DKE, PRL 127, 197701 (2021).

Ongoing research & open questions in MATBG

- Hierarchy of correlated insulators ν = 1 vs. ν = 2.
- Pseudo-gap and quantum critical point.
- Nature of the strange metal phase.
- Pairing symmetry and origin of the SC phase.
- Improved assembly of TBG.

IVC and SC gaps at ν = -2-δ:

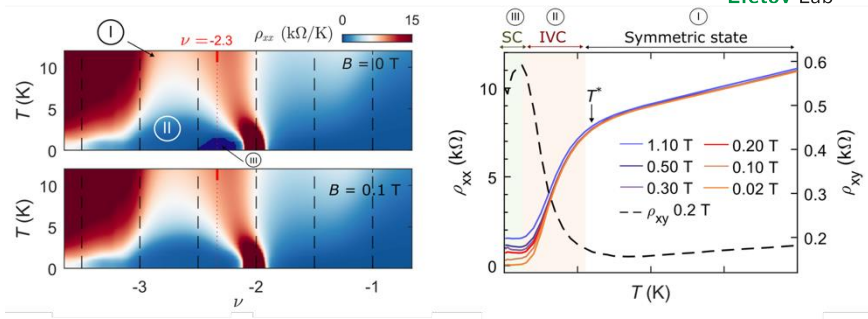

G. diBattista, … , DKE, in preparation.

Linear R vs. T in broad density ranges:

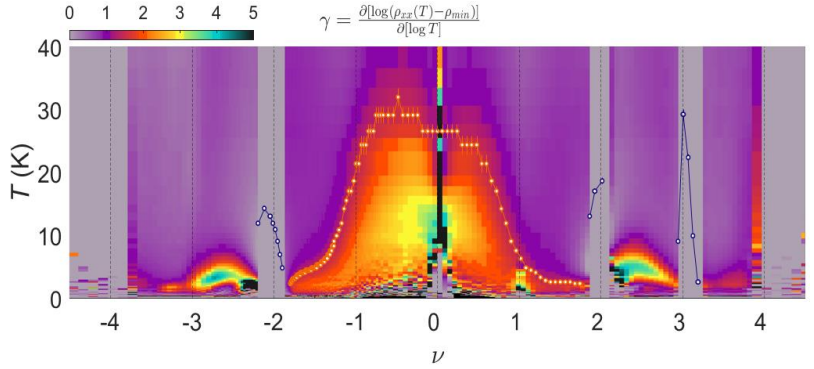

G. diBattista, … , DKE, in preparation.

Noise reveals SC pairing symmetry:

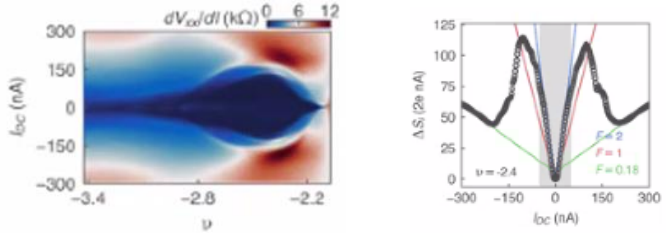

R. Ayache, G. diBattista, … , DKE, P. Rolleau, in preparation.

Engineering topological flat bands in 2D materials

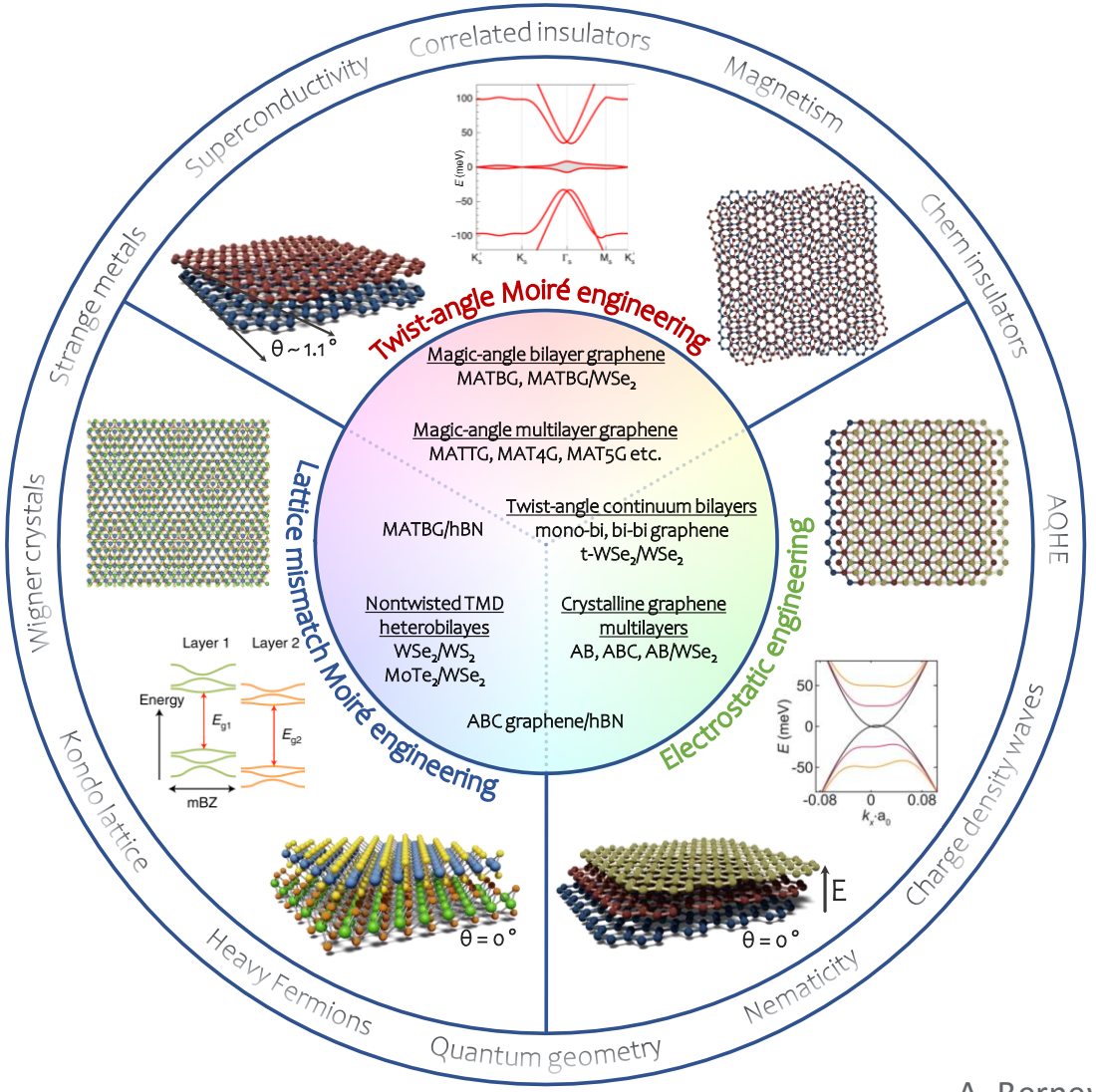

A. Bernevig, DKE, **Physics Today, 77 (4), 38 (2024).**

Engineering topological flat bands in 2D materials
Large library of twistable materials

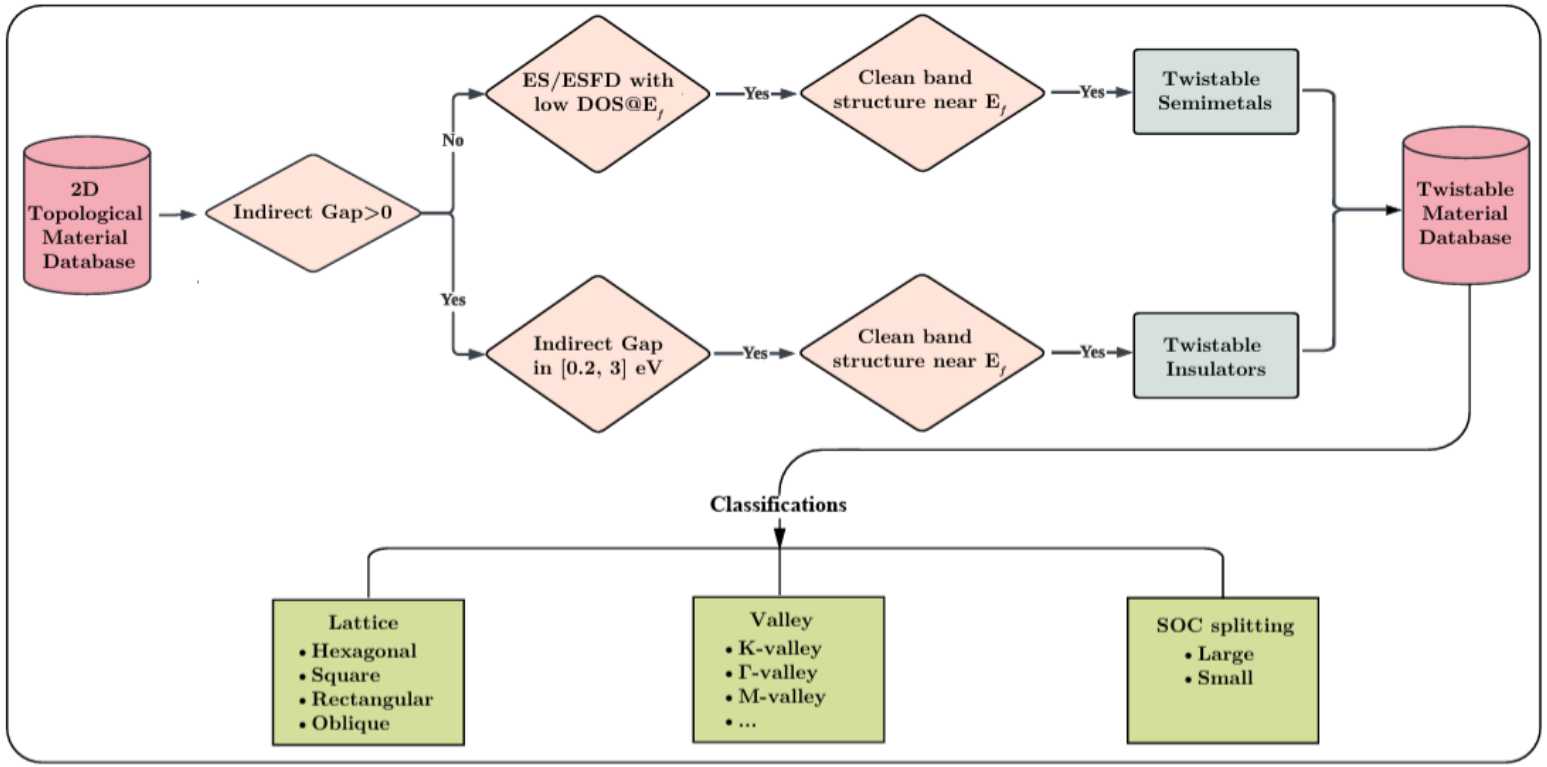

Jiang et al., Science – in press, arXiv:2411.09741 (2024).

- → High-throughput algorithm used to search for 2D twistable materials.
- → Identification of thin film SCs that are gate tunable, clean, single crystals.
- → Simple, isolated bands close to energy gap.
- → Novel real and momentum space symmetries, novel interaction terms.

M- and Γ- point twisted materials

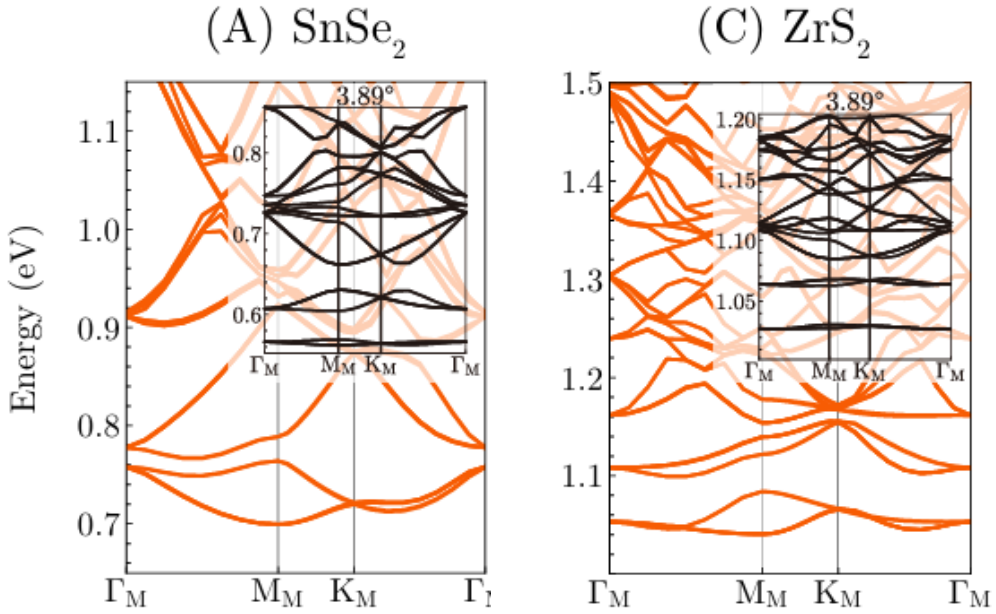

nature

Moiré materials based on M-point twisting

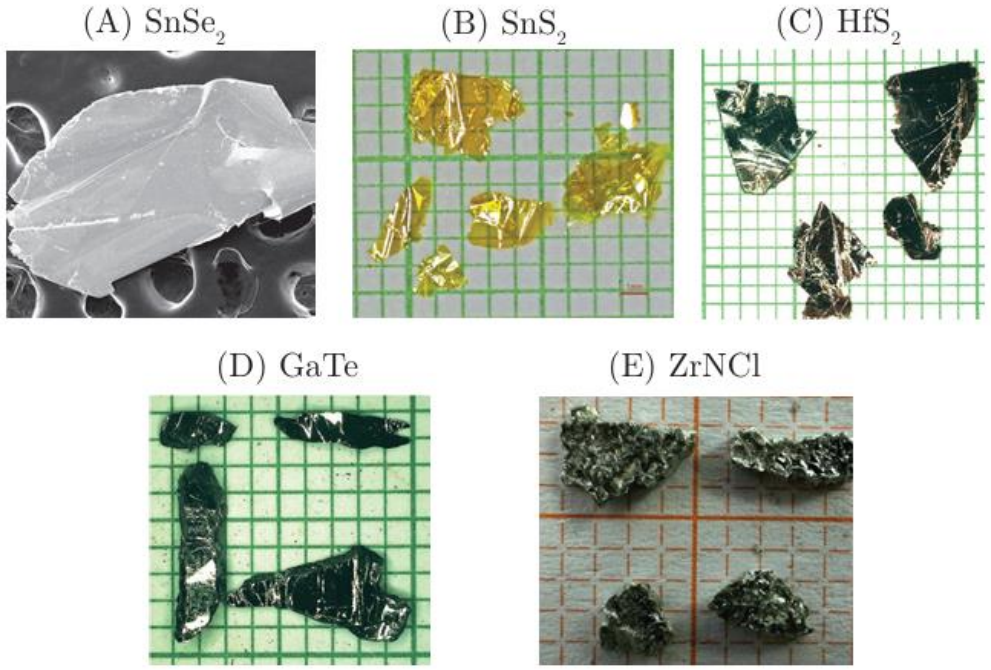

Călugăru et al., Nature 643, 376 (2025).

→ 3 valleys vs 1-2 in conventional systems → richer physics.

→ Ultra-flat bands: Better than most K-point systems
→ stronger correlations.

→ Kagome momentum lattice → creates exotic quantum states naturally.

→ New quantum phases → access to Luttinger liquids and spin liquids.

High throughput assembly and characterization

Efetov Lab

Brookhaven National Laboratory Quantum Press

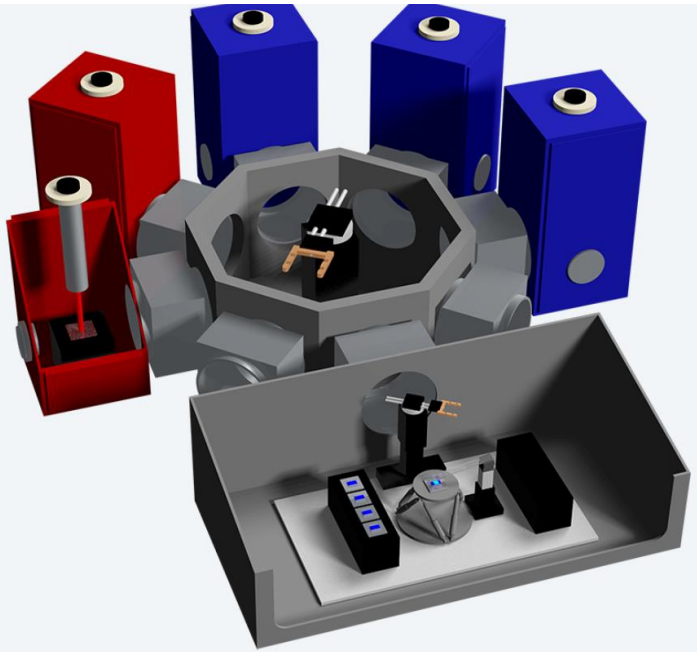

QPress is a modular system

The QPress cluster tool robotically transfers substrates through an integrated sequence of synthesis, processing, and characterization stations. This tool features three custom-built modules: an exfoliator, cataloger, and stacker, each designed for robotic control and automation. This setup enhances the efficiency and reproducibility of synthesizing 2D heterostructures.

The cluster is equipped with:

- **Sample Libraries**: These allow for the storage and retrieval of substrates and intermediate samples under vacuum conditions.
- **Deposition Methods**: Includes an electron-beam system capable of handling various target materials.
- **Pre-/post- Processing Methods**: Features vacuum/argon annealing and oxygen plasma cleaning/etching.
- **Characterization Methods**: Comprises optical microscopy, Raman spectroscopy, photoluminescence spectroscopy (PL), and atomic force microscopy (AFM).

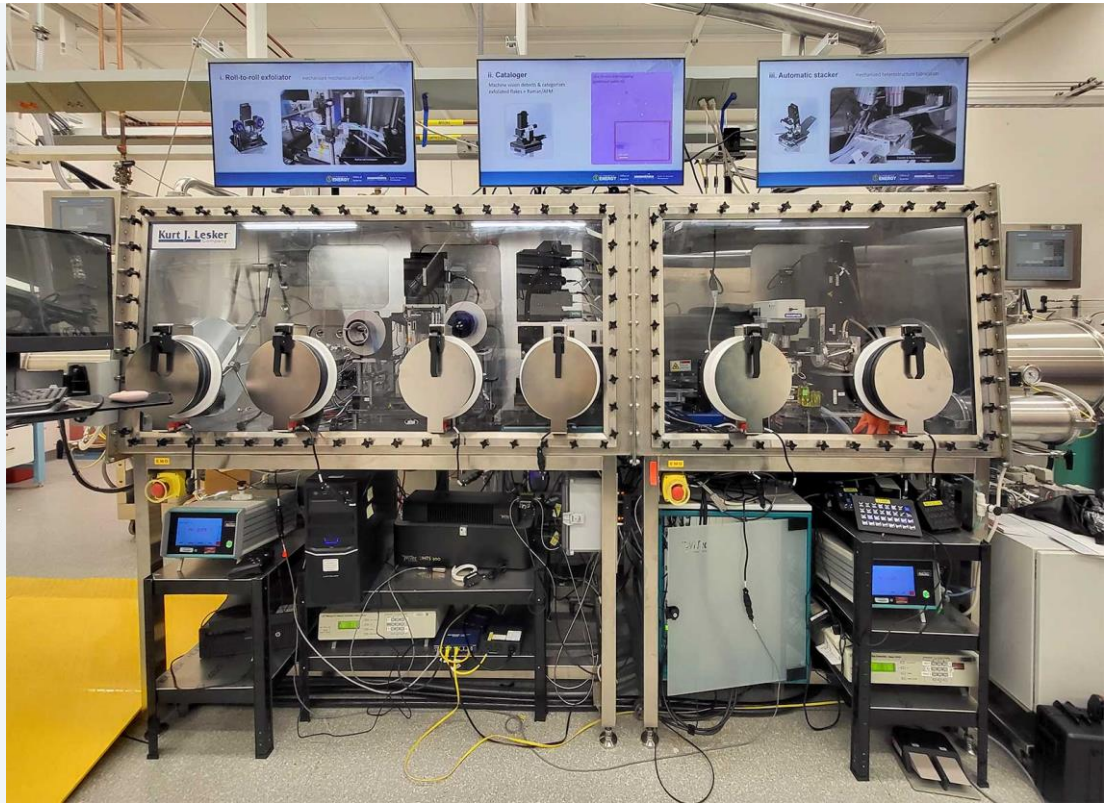

→ Introducing advances in automation and AI in sample preparation, characterization and analysis.

→ Fully automated, AI driven cluster tools are currently built in many places including Brookhaven etc.

Quantum Twisting Microscope (QTM)

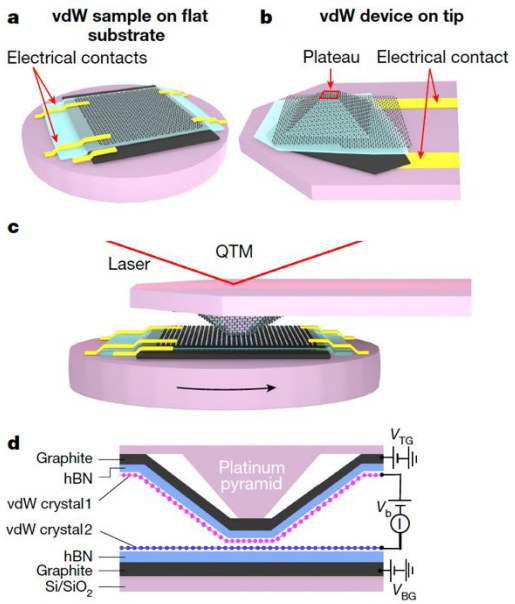

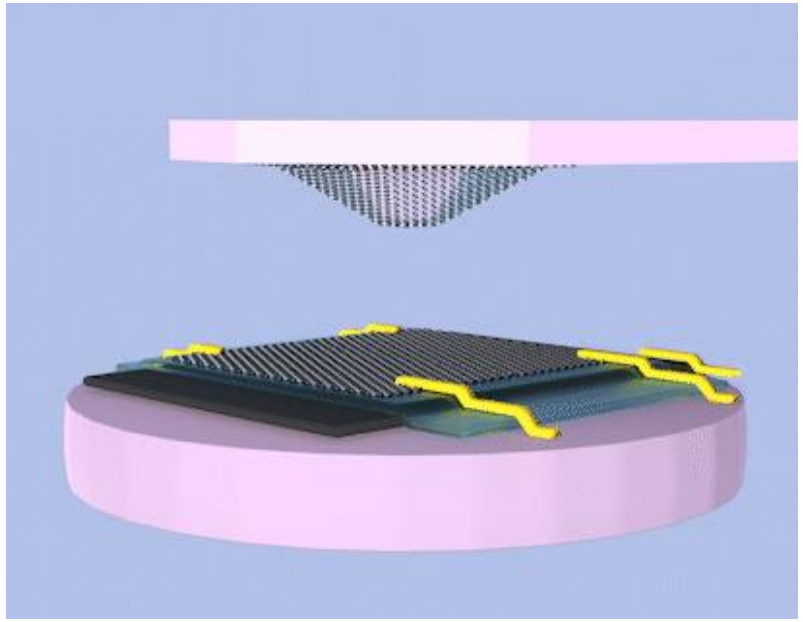

→ Simultaneous preparation and direct measurement of the electronic properties of the moiré hetero-structure.

→ Dynamic twist angle control → fast, homogeneous and reproducible.

→ k-resolution through twist angle → mapping of bands and collective modes.

A. Inbar, … , S. Ilani, Nature 614, 682-687 (2023).

Quantum Twisting Microscope (QTM)

ARPES:

Momentum-ressolved electronic states

QTM:

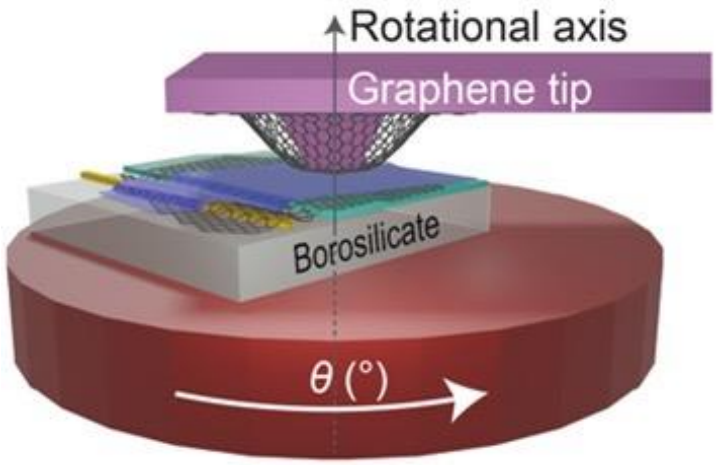

Bridging the gap between ARPES and STM

- → Compatible with mK temperatures and high B-fields.
- → Ultra-high energy resolution < 100µeV, limited only by noise and temperature.
- → Allows imaging above Fermi energy.
- → Compatible with encapsulated and top gated devices.

STM:

Atomic-scale spatial resolution

LMU QTM setup

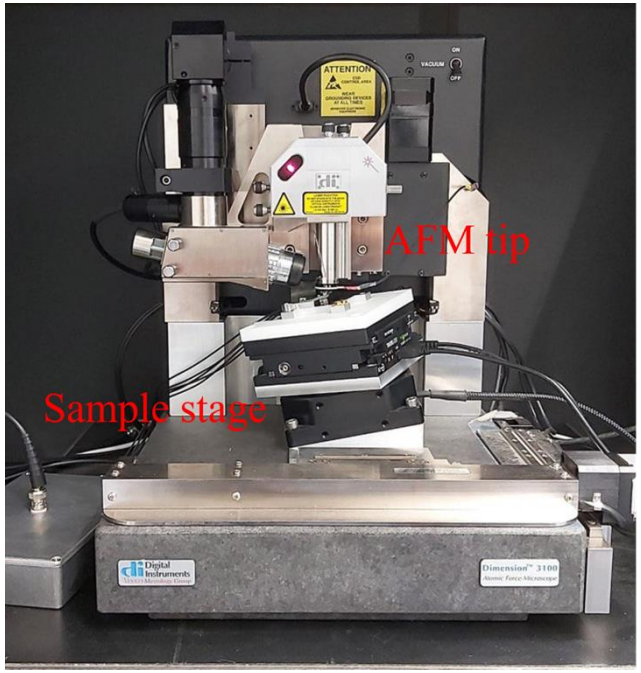

- Modified Dimension 3100 AFM set up.
- Sample stage is inclined at ~ 11º.

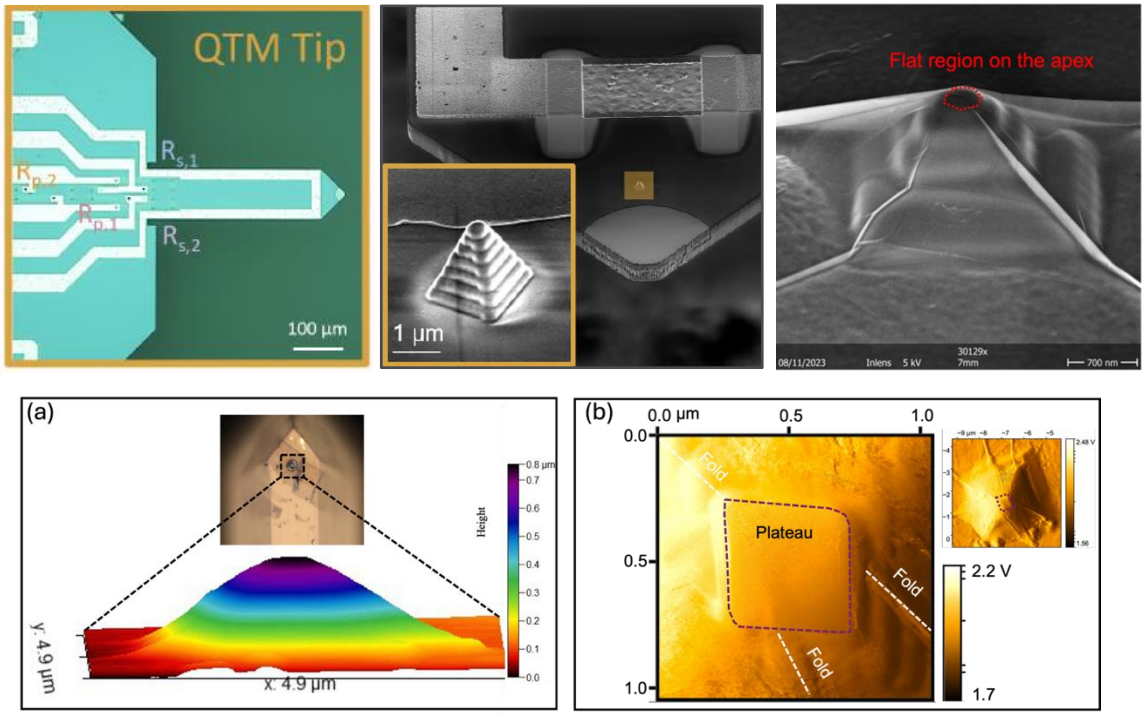

- Home made AFM tips with FIB deposited pyramids, with flat apex ~ 200nm.
- Self-sensing piezo-resistive cantilevers.

M. Lee, I. Das, … , DKE, **Nano Letters (2026).**

Dilution Refrigerator for LT-QTM

QTM tips

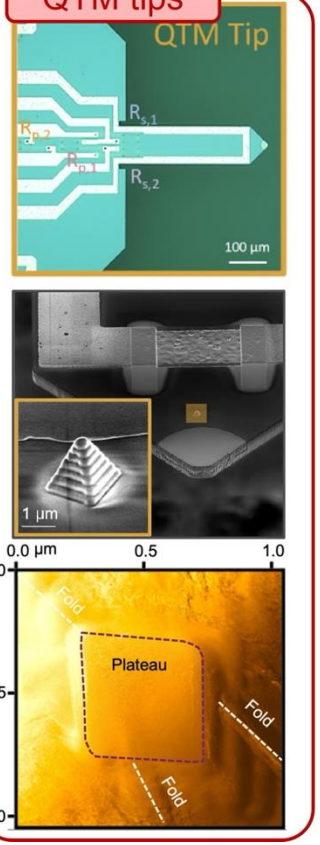

QTM Insert

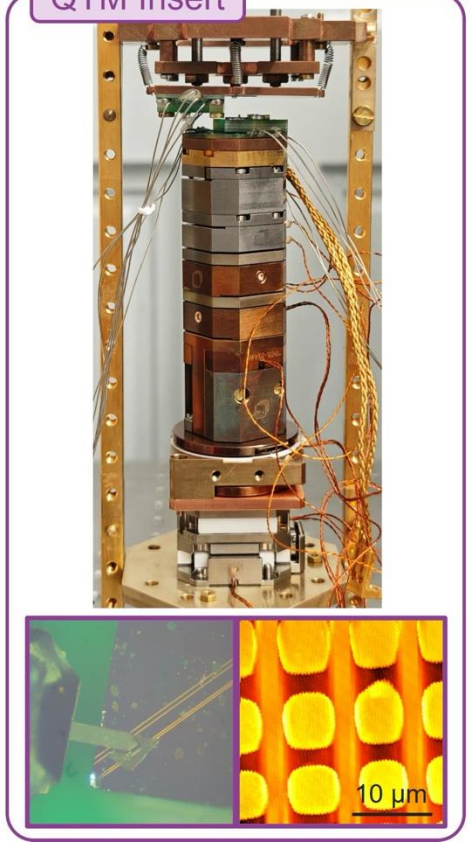

Control Unit

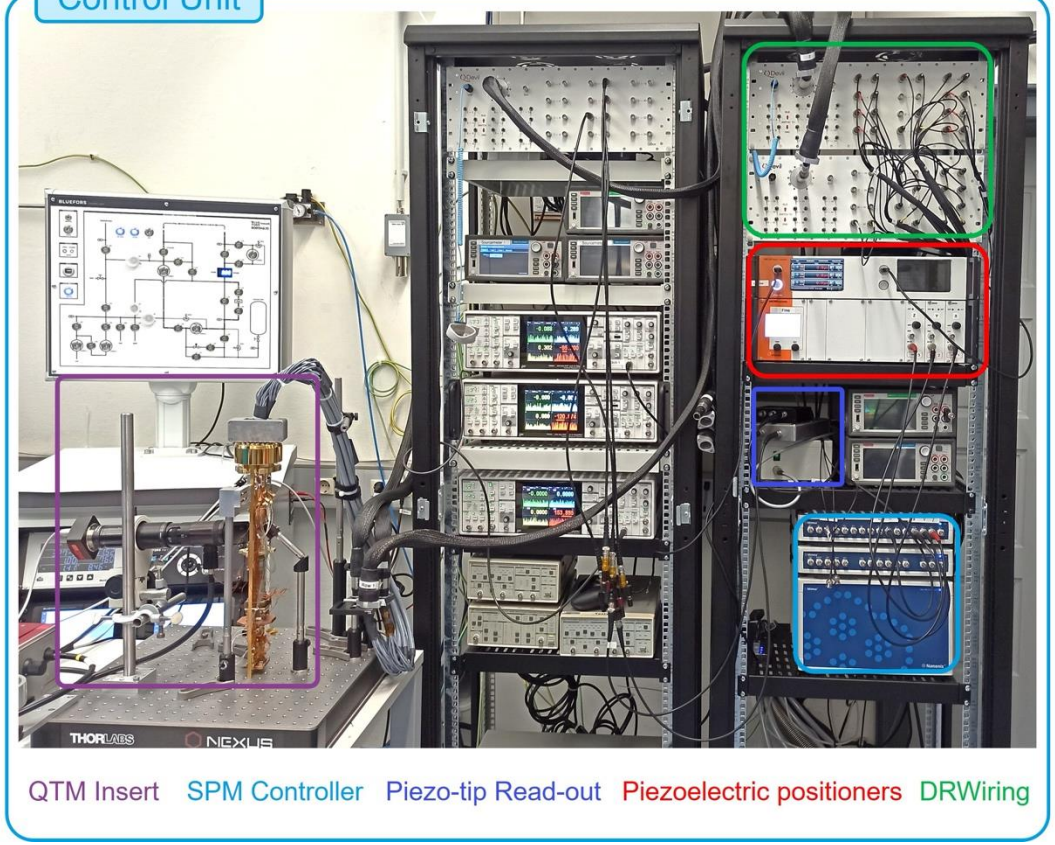

DR

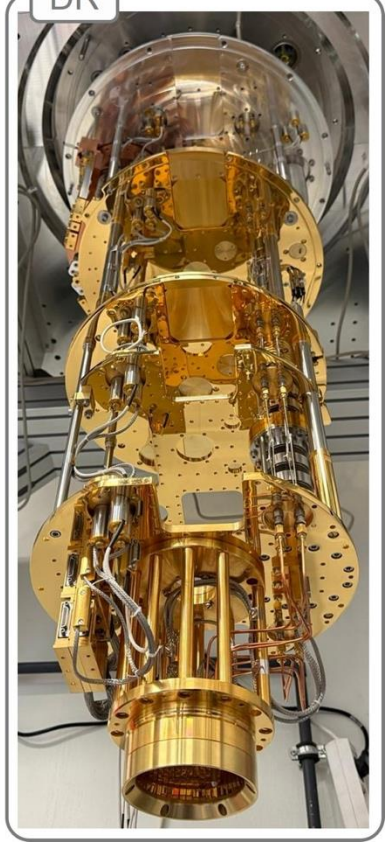

Tunnelling measurement scheme

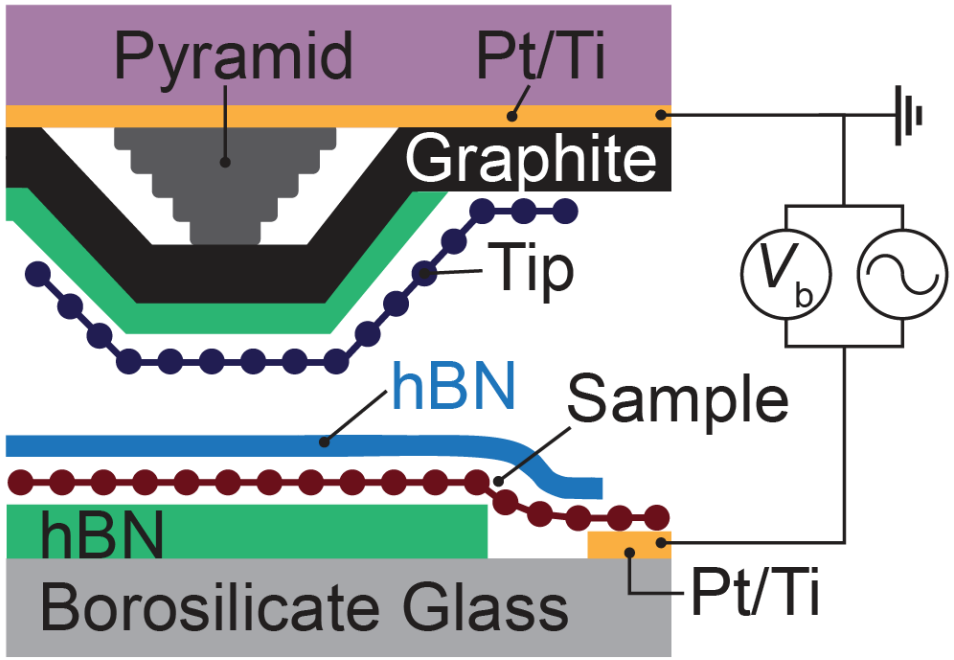

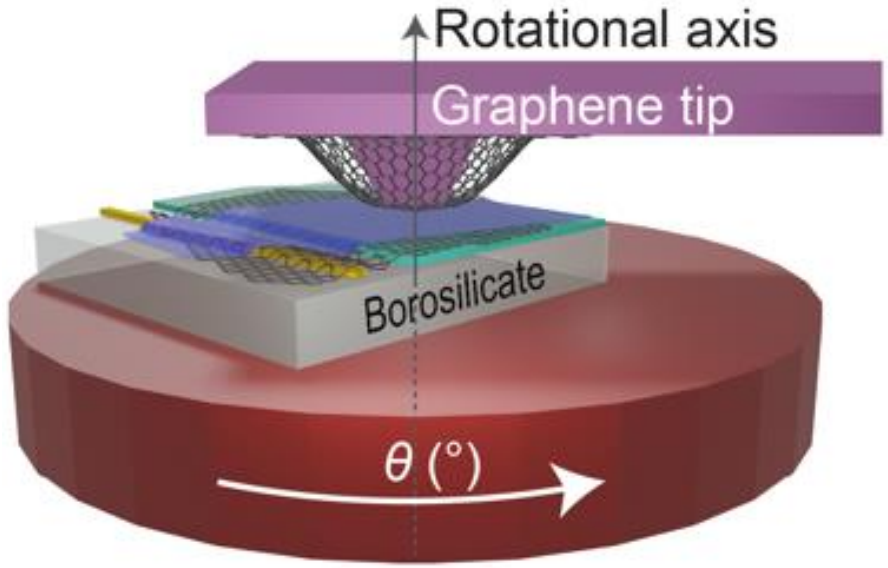

- Graphene coated tip.
- 1-3 layer hBN covered graphene.
- I/V and dI/dV vs. bias voltage V_b tunneling.

M. Lee, I. Das, … , DKE, **Nano Letters (2026).**

Twist-angle dependent tunnelling scheme

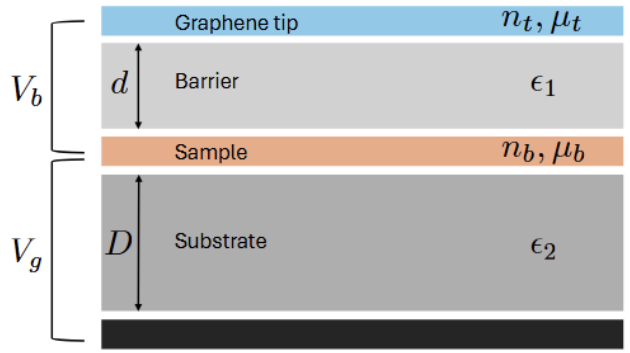

$$-\epsilon_1 E_1 = e n_t$$

$$eV_b = eE_1 d + \mu_b(n_b) - \mu_t(n_t)$$

$$\epsilon_1 E_1 - \epsilon_2 E_2 = e n_b, \quad E_2 = V_g/D$$

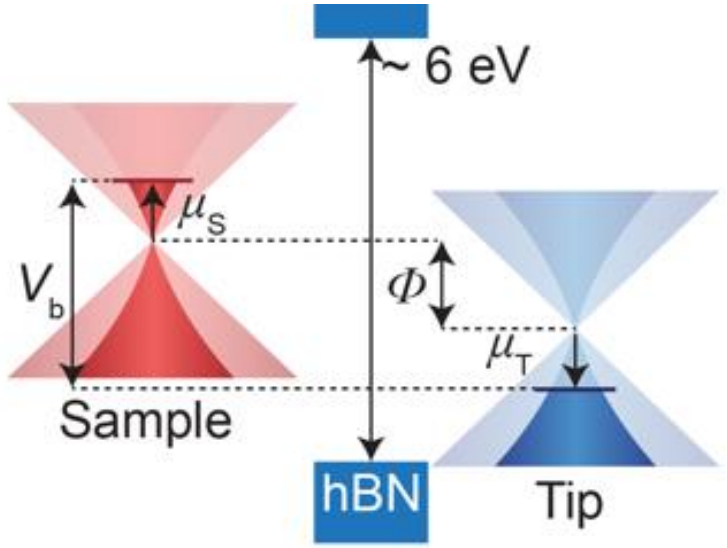

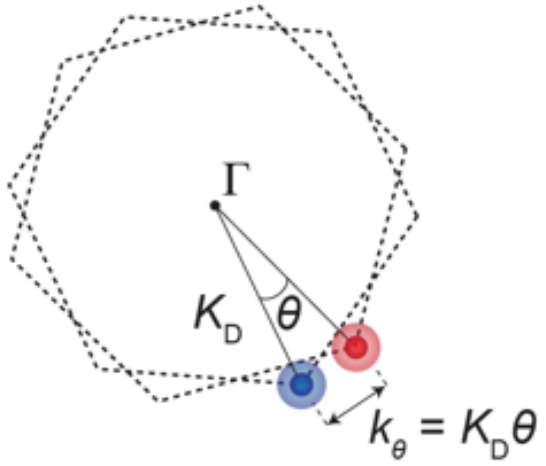

- Energy resolution → voltage bias V_b shift symmetrically the chemical potential μ of graphene layers.
- k-space resolution → twist-angle θ translates into k-space rotation $k_\theta = K_D\theta$.

M. Lee, I. Das, … , DKE, **Nano Letters (2026).**

SLG/hBN/SLG tunnelling spectra

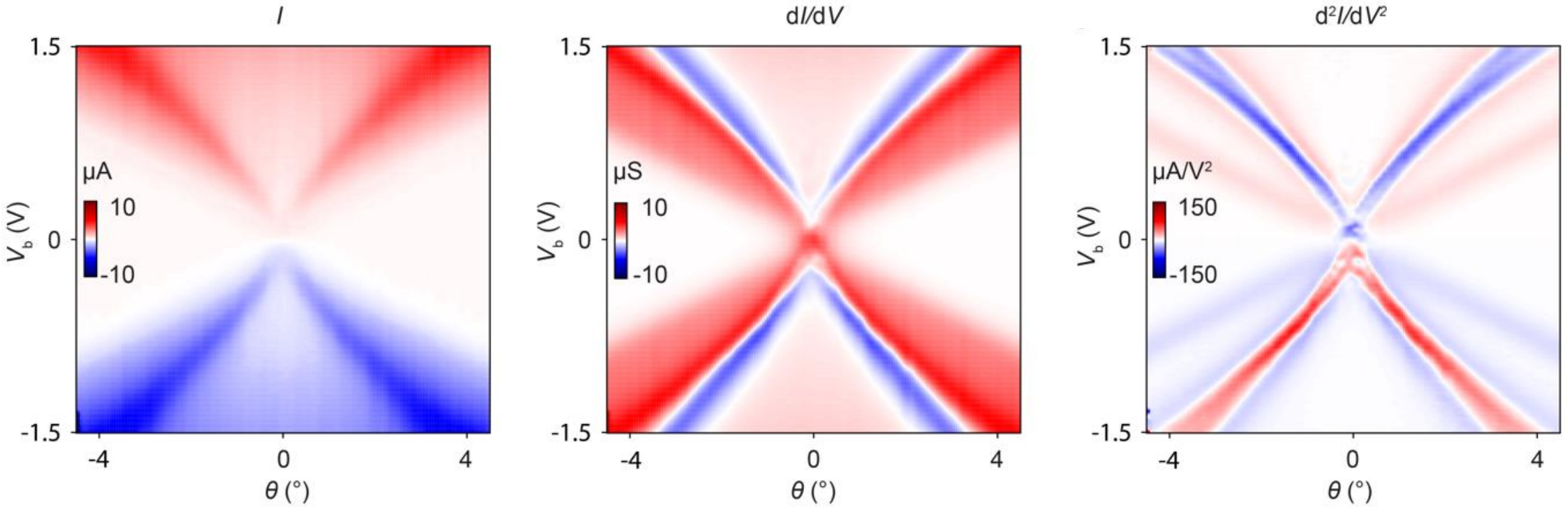

M. Lee, I. Das, … , DKE, **Nano Letters (2026).**

Onset and nesting conditions

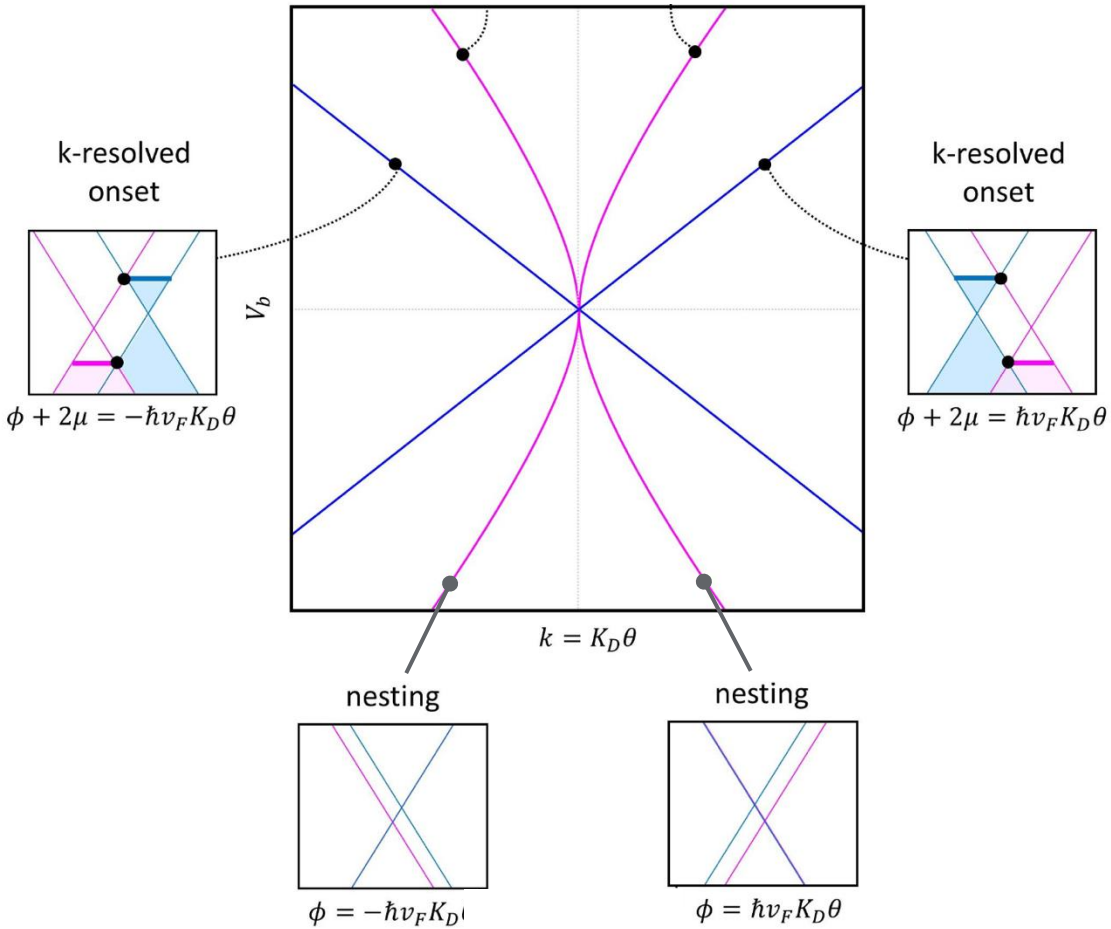

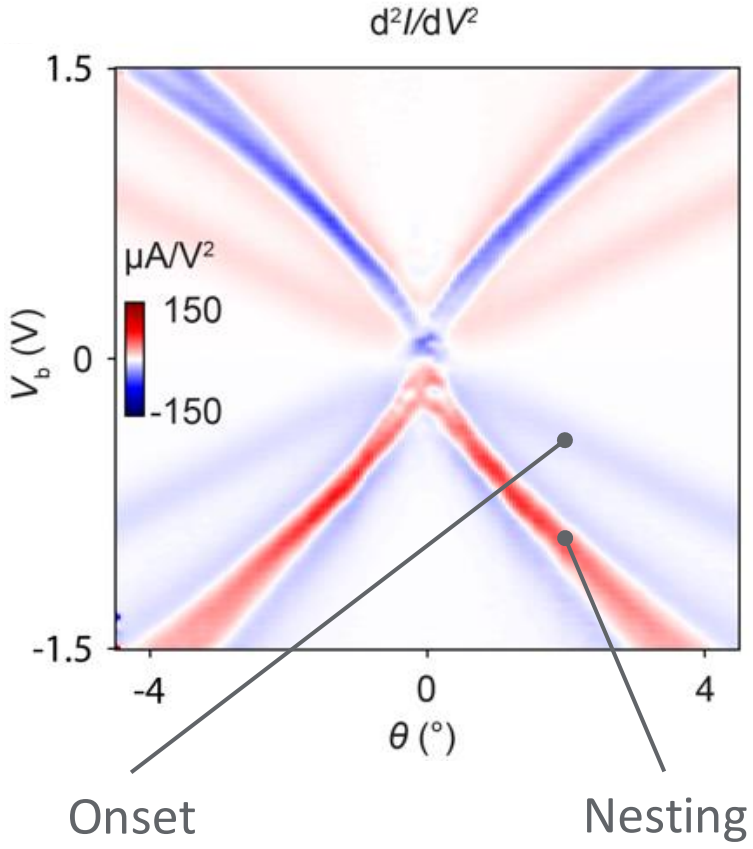

$V_b = \pm \hbar v_F K_D \theta$ $\Phi = \pm \hbar v_F K_D \theta$

A. Inbar, … , S. Ilani, **Nature 614, 682-687 (2023).**

M. Lee, I. Das, … , DKE, **Nano Letters (2026).**

Electron-electron renormalized Dirac cones

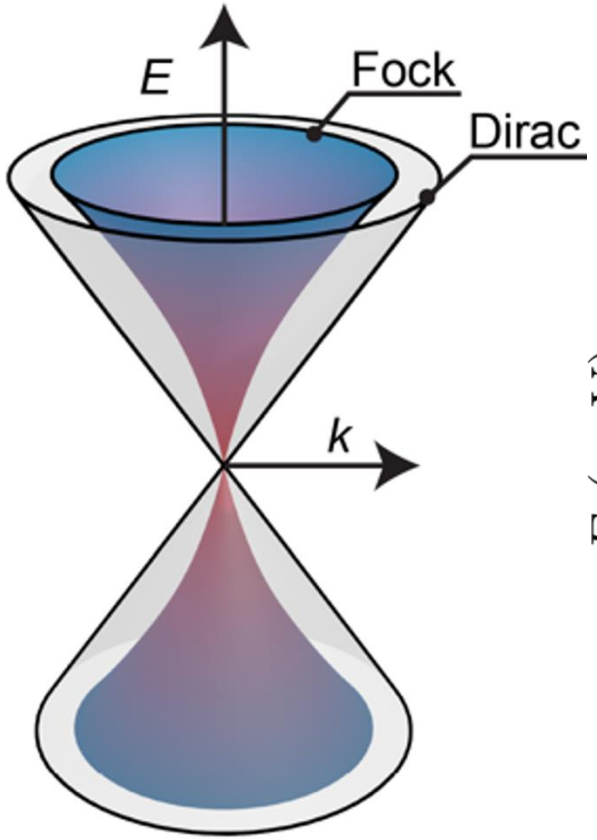

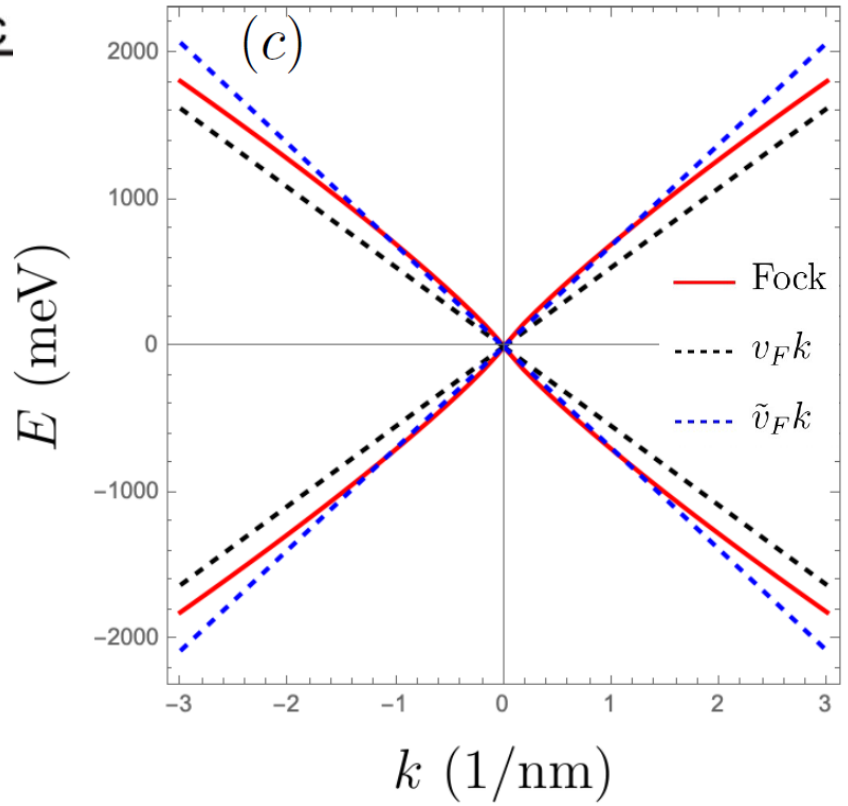

- Dirac → $E = \hbar v_F k$

  Typically v_F ~ 1.05 x 10^6 m/s

- Fock → $E = \pm\hbar v_{\mathrm{F}}^0 k\left(1 + \frac{\alpha}{4}\ln\left(\frac{\Lambda}{k}\right) + \frac{\alpha}{4}\right)$

  Typically v_{F}^0 ~ 0.85 x 10^6 m/s

  α ~ 0.05 – 1 – graphene's fine structure constant → e-e interaction strength.

M. Lee, I. Das, … , DKE, **Nano Letters (2026).**

SLG/hBN/ABC trilayer tunneling spectroscopy with D

ABA trilayer graphene QTM·

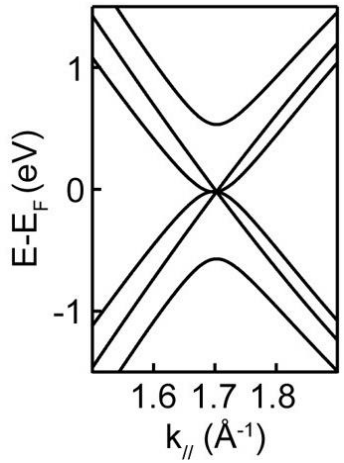

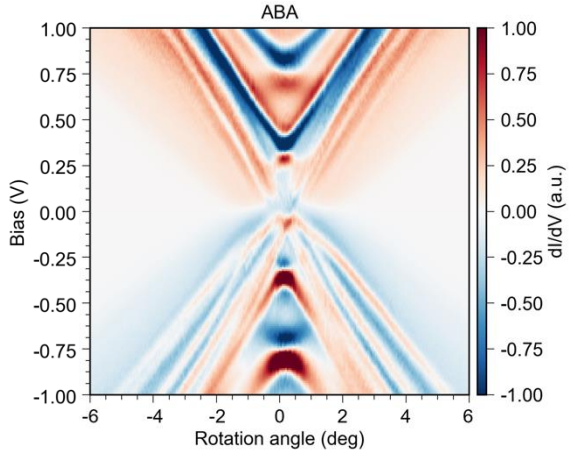

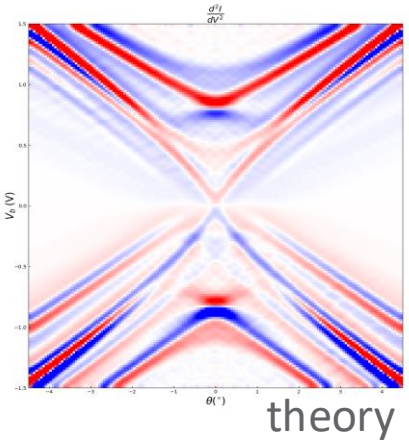

ABA ARPES:

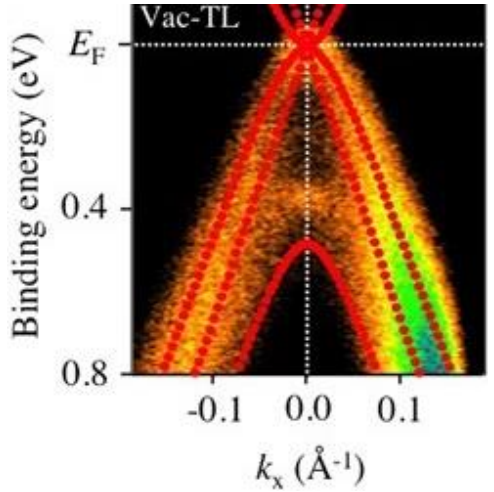

ABC trilayer graphene QTM:

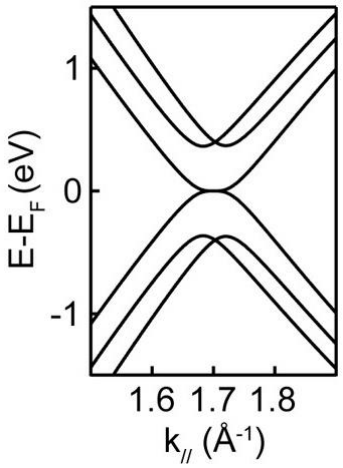

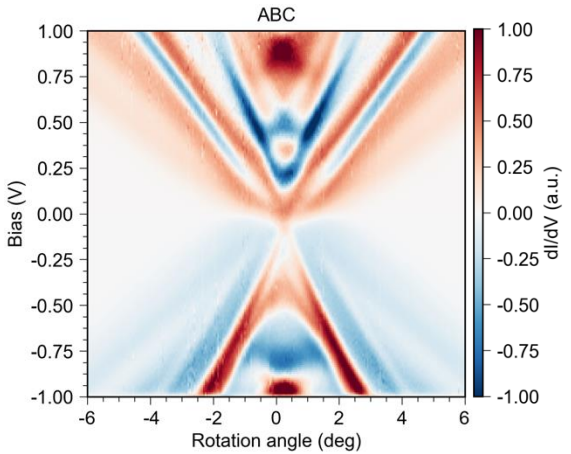

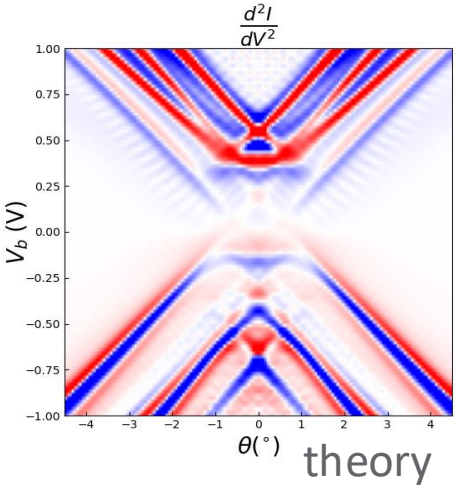

ABC ARPES:

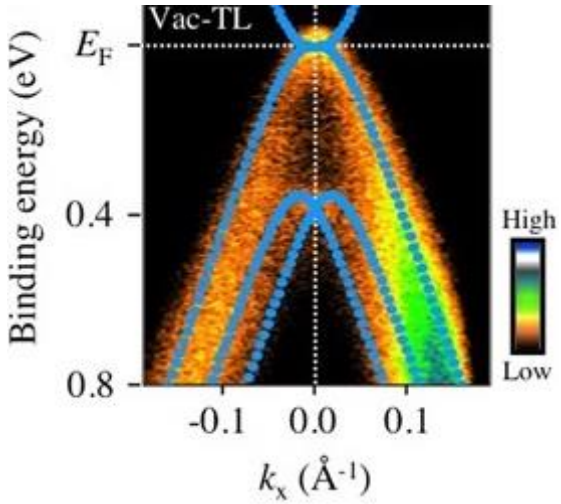

Next steps for QTM

→ Explore twist-angle dependent phase-diagrams of library of 2D materials.

→ Map SC order parameter & spectral diffusion in strange metal phase of MATBG.

→ Probe ABC graphene under displacement field, including spectral functions of FCI states.

→ Use phase-sensitive QTM tunnelling to interferometrically couple to topological edge states.

Library of moiré materials:

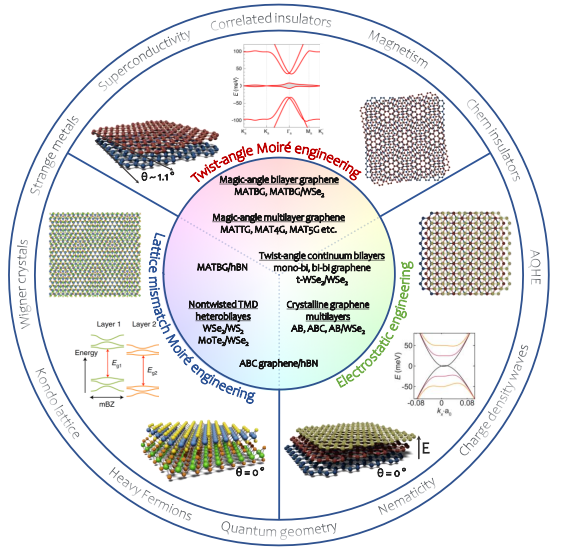

A. Bernevig, DKE, Physics Today, 77 (4), 38 (2024).

Mapping TBG spectra:

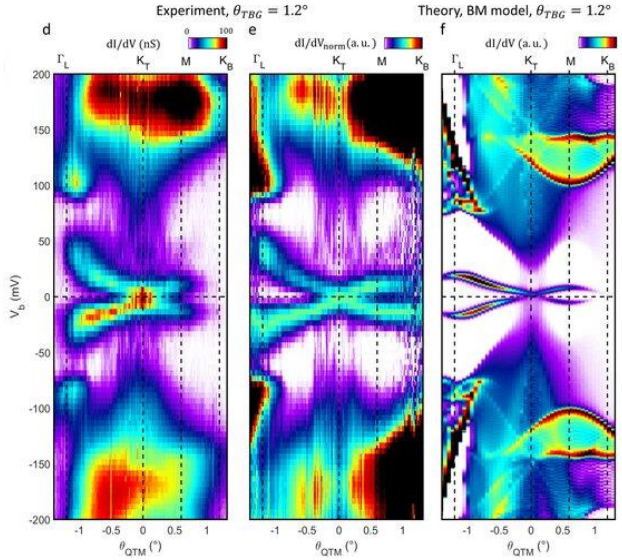

Ilani group (2025).

LMU LUDWIG-MAXIMILIANS-UNIVERSITÄT MÜNCHEN

Efetov Lab
Chair of Quantum Materials

Thank you for your attention!

Correlated insulators

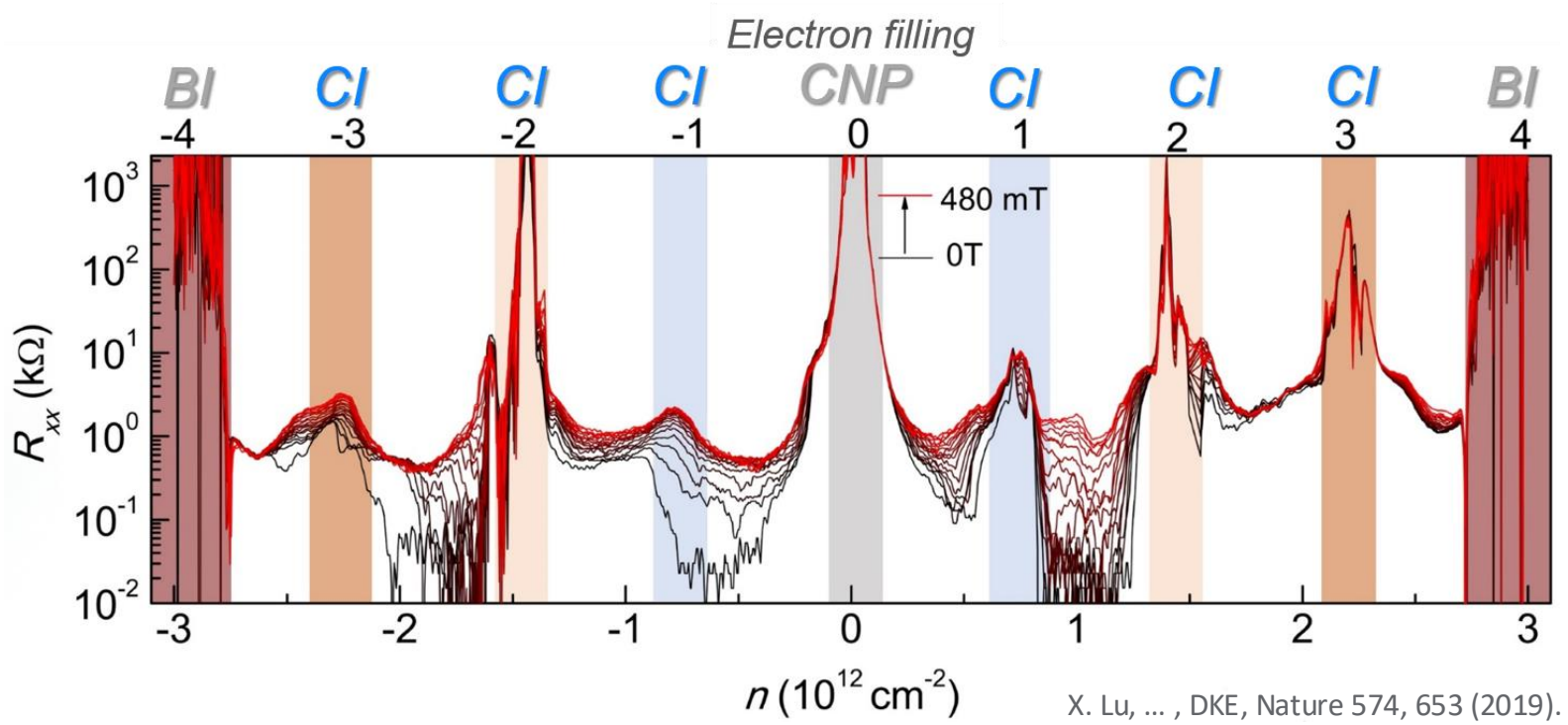

X. Lu, … , DKE, Nature 574, 653 (2019).

Symmetry broken correlated insulators at all integer fillings ν = 0,±1,±2,±3 e/uc

Mott insulator picture

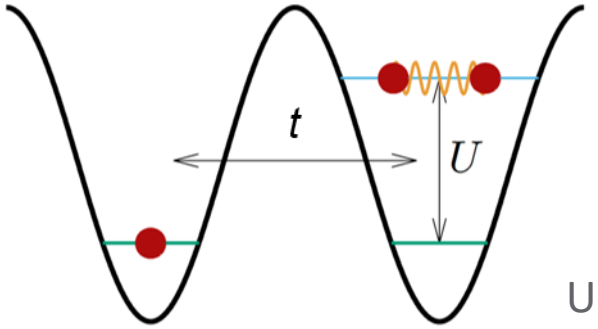

U – onsite energy (Coulomb)

$$U = e^2\theta/(4\pi\varepsilon_0\kappa a)$$

$$H = -t\sum_{i,j,\sigma} c^{\dagger}_{i,\sigma}c_{j,\sigma} + U\sum_{i} n_{i,\uparrow}n_{i,\downarrow}$$

partial filling - correlated metal:

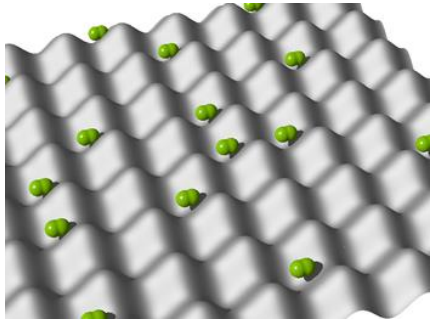

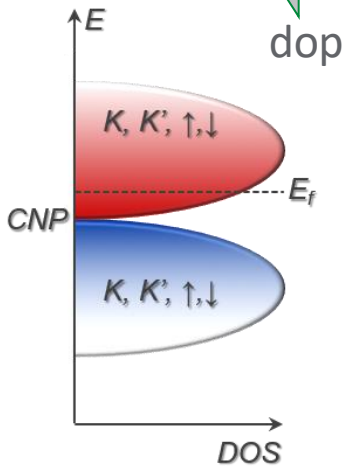

doping

integer filling – Mott insulator:

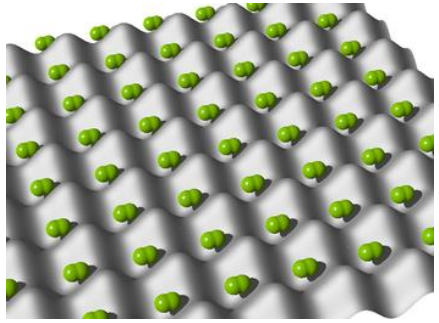

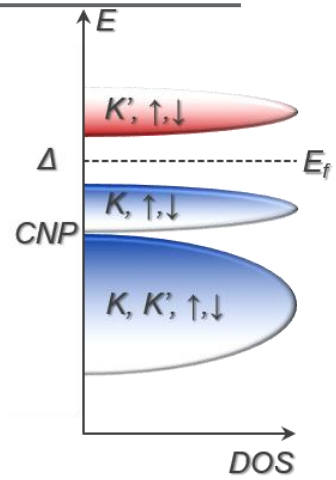

U/t >> 1

SU(4) spin/valley symmetry breaking

Correlated Chern insulators in B-field

Chern insulators in B-field - Streda Formula:

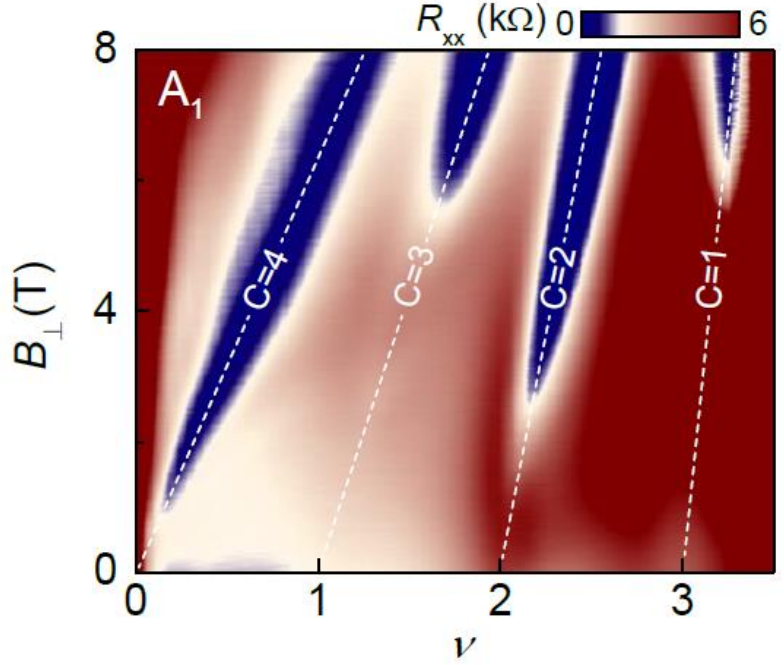

I. Das, X. Lu, … , DKE, Nature Physics 17, 710 (2021).

Quantized Hall conductance:

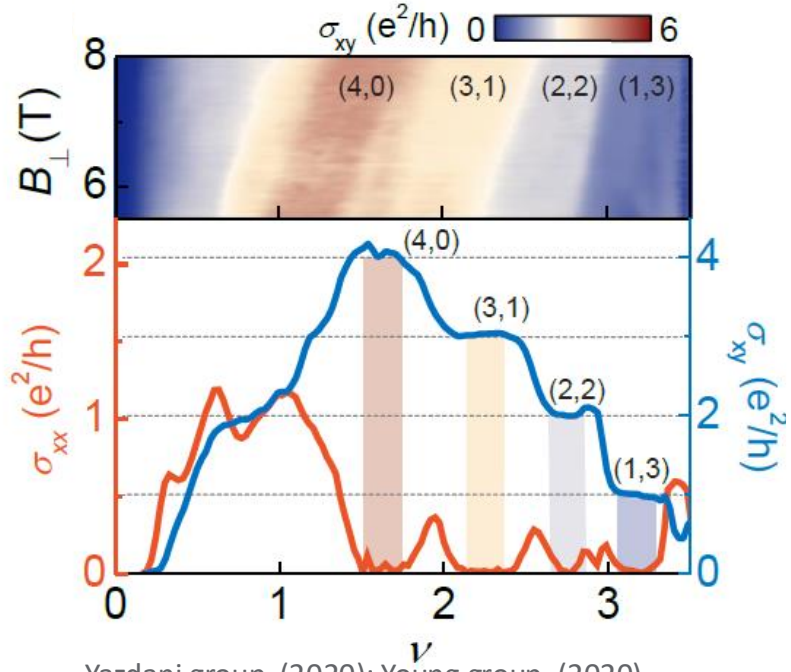

Yazdani group, (2020); Young group, (2020).
Nadj-Perge group, (2020); Andrei group, (2020).
Jarillo-Herrero group, (2020).

Energy gaps: CCI (1meV) >> LL (0.1meV)
Quantization field: CCI (0.3T) << LL (3T)
STM: interaction induced gaps show spectral broadening

Orbital magnetism at zero B-field

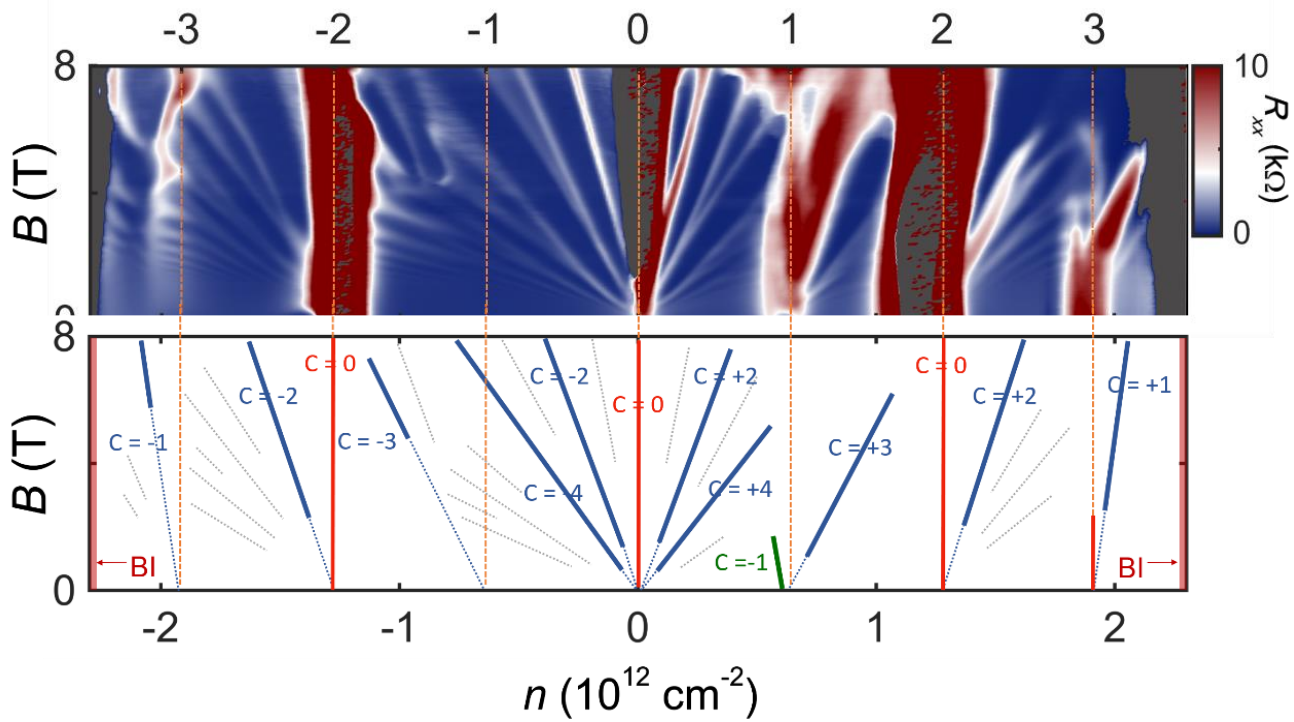

Hystheretic B-field dependence:

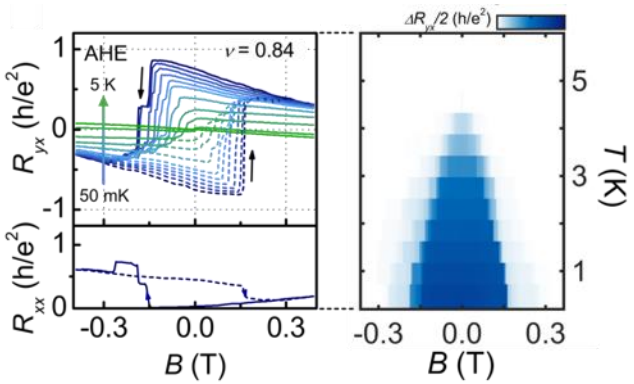

Orbital Magnetism → valley polarization:

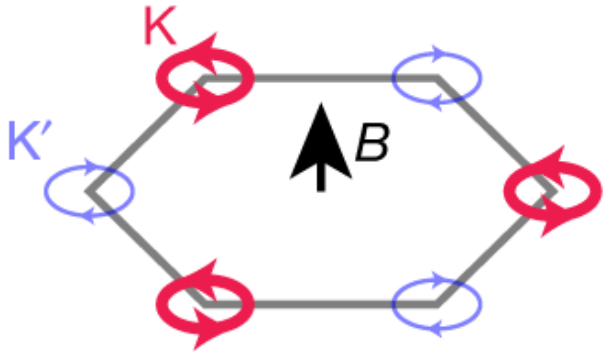

P. Stepanov, … , A. Bernevig, DKE, PRL 127, 197701 (2021).

Unconventional SC in MATBG?

Efetov Lab

Flat bands:

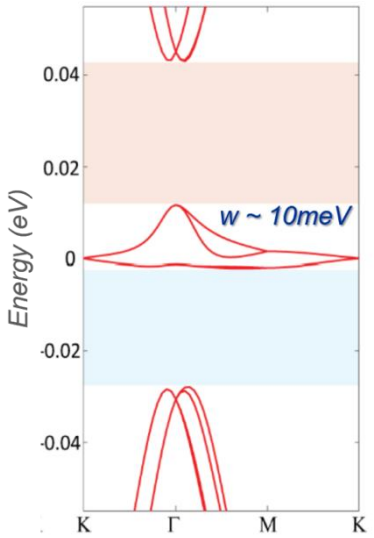

H. Yoo, … , E. Kaxiras, P. Kim, **Nat. Mat. 18, 448 (2019).**

Phase diagram:

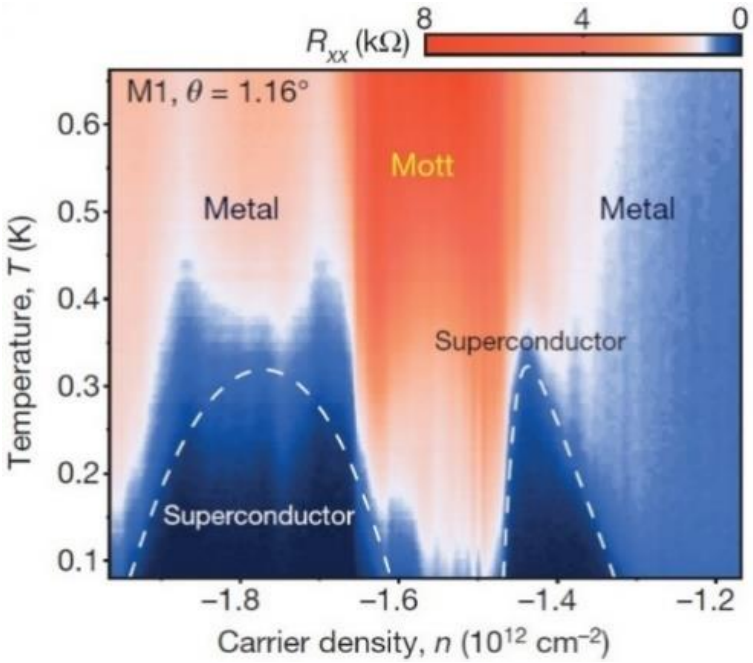

Y. Cao, … , P. Jarillo-Herrero, **Nature 556, 43–50 (2018).**

Uemura plot:

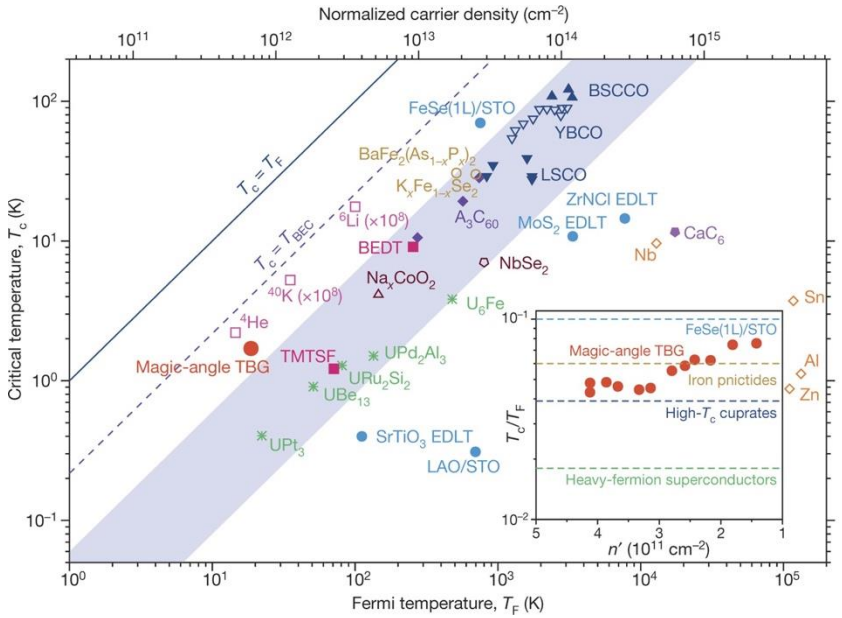

- Similar phase diagram to the cuprates.
- Record strong coupling – defined by $T_c/T_f \sim 0.1$.
- Record low carrier density of any superconductor.
- Proximity to CI states – non e-ph mechanism?

Characterization of the SC state

Efetov Lab

Critical temperature T_C:

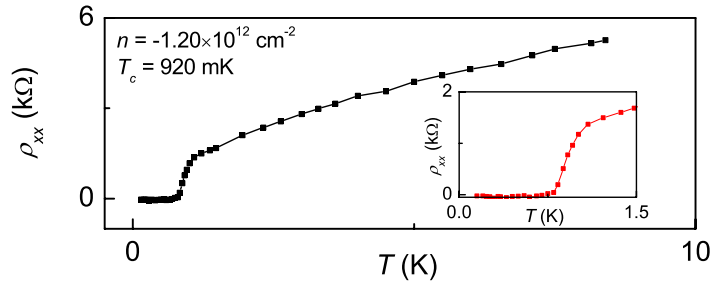

Critical B-field B_C:

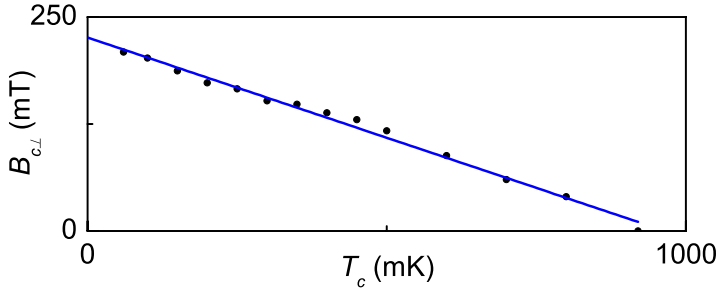

Critical current I_C:

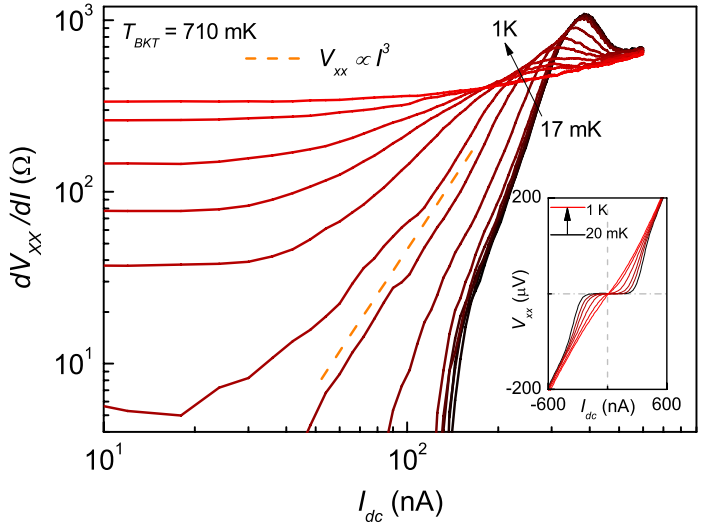

Frauenhofer interference (disorder):

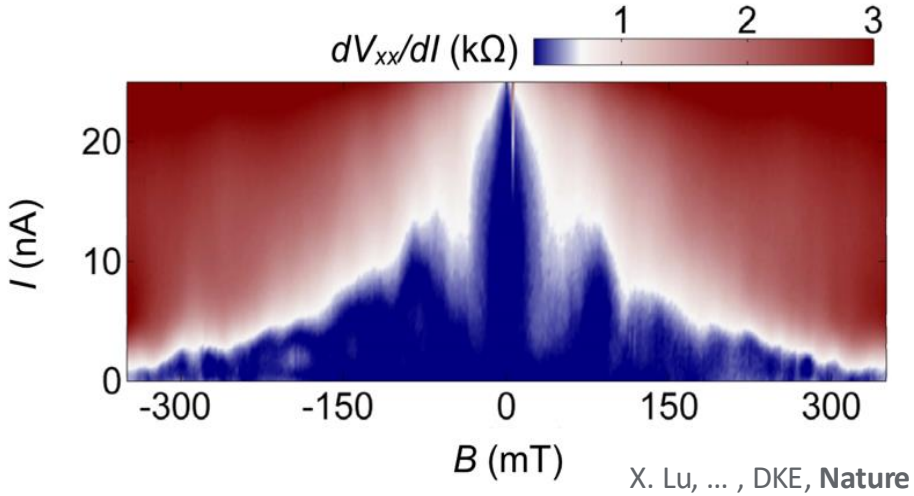

X. Lu, … , DKE, **Nature 574, 653 (2019).**

Consistent with GL and BKT → T_c ~ 1K, H_c ~ 100mT, I_c ~ 10nA, ξ ~ 50nm

Nodal SC pairing mechanism?

STM tunneling spectroscopy:

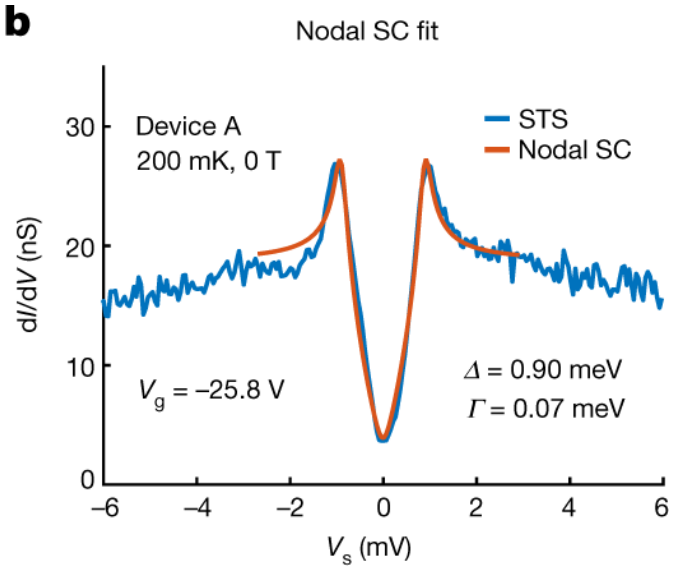

- Observation of V – shaped gaps.

M. Oh, … , Ali Yazdani, **Nature 600, 240–245 (2021).**
H. Kim, … , Stevan Nadj-Perge, **Nature 606, 494–500 (2022).**

T-dep. thermal conductivity:

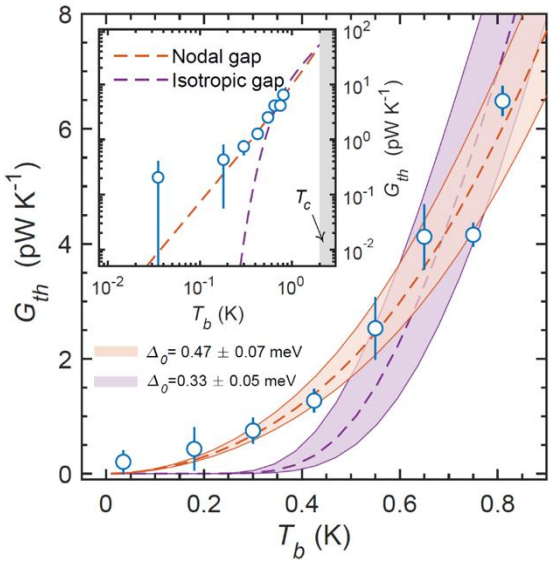

- Power-law T-dependence of thermal conductivity.

G. Di Battista, … , K. C. Fong, DKE, **Nano Letters 22, 16 (2022).**

T-dep. superfluid stiffness:

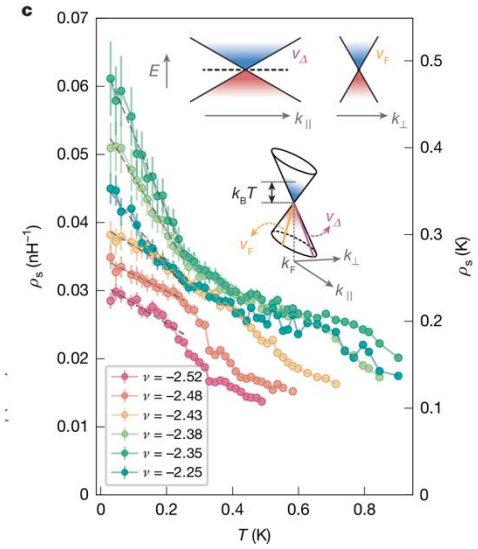

- Linear T-dependence of superfluid stiffness.

M. Tanaka , … , W. D. Oliver, **Nature 638, 99–105 (2025).**
A. Banerjee, … , P. Kim, **Nature 638, 93–98 (2025).**

Linear T-dependent resistivity

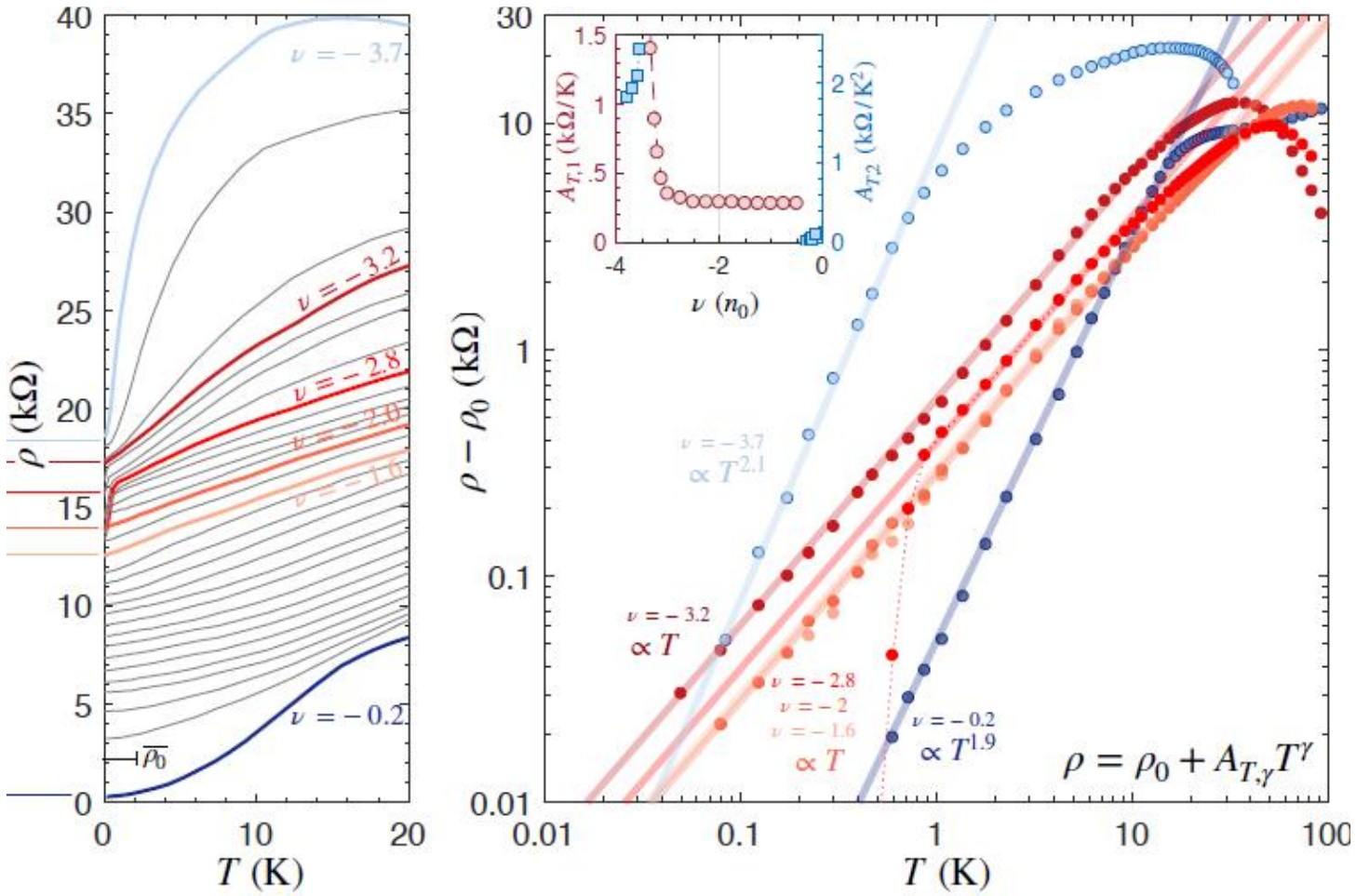

→ Linear R vs. T over 3 orders and down to T=40mK

A. Jaoui, … , L. Levitov, DKE, Nature Physics 18, 603 (2022).

Linear B-dependence and Planckian scattering rate

R vs. B-dependence:

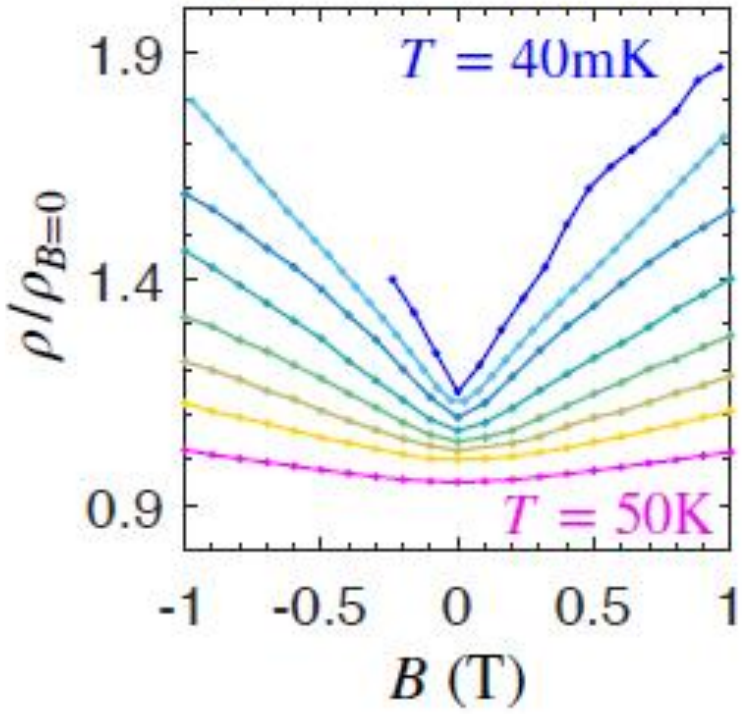

Planckian scattering rates:

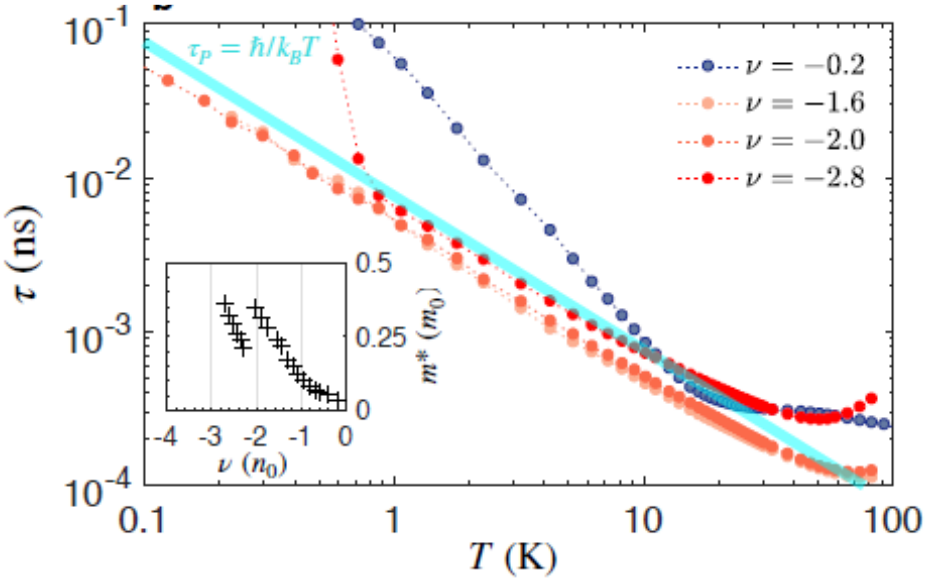

$$\tau \sim \tau_P = \hbar / k_B T$$

→ Ranges of linear T- and B-dependence and Planckian scattering rate coincide

Strange metal - parent state of the SC state

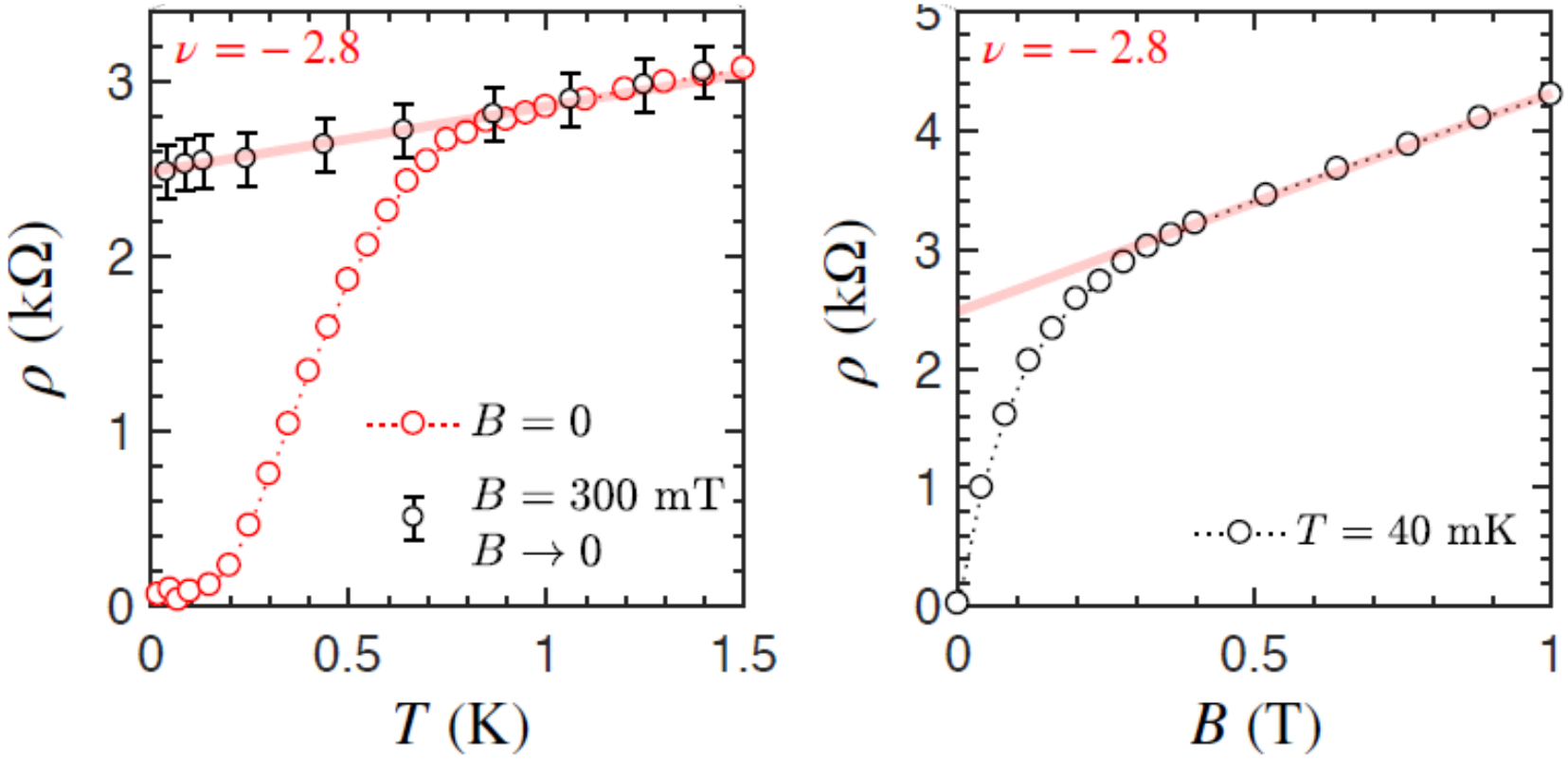

→ Density ranges of linear T- and B-dependence coincide

→ Energy scales of linear behavior in T and B coincide

Farbübersicht

Efetov Lab

R 0 G 136 B 58	R 35 G 35 B 35	R 255 G 255 B 255
LMU Grün	Schwarz	Weiss

R 15 G 25 B 135	R 100 G 59 B 227	R 140 G 64 B 145	R 215 G 25 B 25
Akzent Blau	Akzent Cyan	Akzent Violett	Akzent Rot

R 241 G 135 B 0
Akzent Orange

R 98 G 100 B 104	R 192 G 193 B 195	R 230 G 230 B 231	R 245 G 245 B 245
Sekundär Dunkelgrau	Sekundär Mittelgrau	Sekundär Hellgrau	Sekundär Lichtgrau